IAEA TRAINING COURSE SERIES No. 16

Neutron and gamma probes: Their use in agronomy

INTERNATIONAL ATOMIC ENERGY AGENCY, VIENNA, 2002

The originating Section of this publication in the IAEA was:

Soil and Water Management & Crop Nutrition Section
International Atomic Energy Agency
Wagramer Strasse 5
P.O. Box 100
A-1400 Vienna, Austria

NEUTRON AND GAMMA PROBES: THEIR USE IN AGRONOMY
IAEA, VIENNA, 2002
IAEA-TCS-16
ISSN 1018–5518

Printed by the IAEA in Austria
August 2002

FOREWORD

Water is an essential requirement for life on the planet. It is often the single most limiting factor in crop and livestock production. Water is a scarce resource in many urban and rural environments worldwide. According to the FAO, the global demand for fresh water is doubling every 21 years. The quality of the finite water supplies is also under threat from industrial, agricultural and domestic sources of pollution.

The majority of crops are grown under rain-fed conditions and adequate water supply is the main factor limiting crop production in semi-arid and sub-humid regions. On the other hand, currently 20% of the world's arable land is under irrigation providing 35 to 40% of all agricultural production. Irrigation mismanagement poses a serious threat to the environment through groundwater pollution and salinization. It is therefore, essential that water resources be used efficiently by regular monitoring of soil-water status in the unsaturated zone. The neutron depth probe, a nuclear-based technique, is utilized worldwide for this purpose. The neutron moisture gauge, since its introduction some 40 years ago, can now be considered a routine method in soil water studies. Many developments have since been introduced, in particular electronic components, which have significantly improved performance and expanded applications. Although the neutron scattering method is routinely utilised in many developed countries, its use is still limited in developing countries due to several factors. Neutron depth probes contain radioactive sources, which will present health and environmental hazards if a probe is improperly used, stored or disposed of. National and international legislation and regulations must be complied with.

The strategic objective of the sub-program Soil and Water Management & Crop Nutrition of the Joint FAO/IAEA Division of Nuclear Techniques in Food and Agriculture is to develop and promote the adoption of nuclear-based technologies for optimising soil, water and nutrient management within cropping systems. In this context, neutron moisture probes in combination with isotope techniques are utilized to obtain precise and quantitative data on water and nutrient dynamics in the soil-plant system.

The Centre for Nuclear Techniques in Agriculture (CENA) of the University of Sao Paulo, Piracicaba, Brazil is an institute established with IAEA support, with skilled and experienced staff and facilities to utilize nuclear techniques in agronomic and related environmental research. Many training events and formal undergraduate and post-graduate courses involving the use of neutron moisture meters have been offered by CENA. The concept of a training manual originated during a regional training workshop on the use of the neutron probe in water and nutrient balance studies, organized in 1997 in the frame of an IAEA Regional Technical Co-operation Project for Latin America entitled Plant Nutrition, Water and Soil Management (RLA/5/036-ARCAL XXII), for which the integrated approach was adopted. The original version (in Spanish) was a comprehensive manual covering theoretical and practical aspects required for the proper utilization of the equipment. The contributions of the peer reviewers, editors and technical translators of the three versions in English, French and Spanish have greatly enhanced the content and quality of the manual. Their assistance and dedication is highly appreciated.

It is hoped that this manual will be useful for future training events and serve as a key reference to soil/water scientists in the field of sustainable management of scarce water resources in both rain-fed and irrigated agricultural production systems.

The IAEA officer responsible for this publication was F. Zapata of the Joint FAO/IAEA Division of Nuclear Techniques in Food and Agriculture.

EDITORIAL NOTE

The use of particular designations of countries or territories does not imply any judgement by the publisher, the IAEA, as to the legal status of such countries or territories, of their authorities and institutions or of the delimitation of their boundaries.

The mention of names of specific companies or products (whether or not indicated as registered) does not imply any intention to infringe proprietary rights, nor should it be construed as an endorsement or recommendation on the part of the IAEA.

TABLE OF CONTENTS

1. INTRODUCTION

Agriculture is carried out on a very thin surface layer of soil, as compared with the dimensions of the atmosphere and geosphere. Despite its slim dimension, soil is indispensable for life, being the substrate for the growth of plants that sustain humans and animals. Without soil, our planet would be other than green, and life would be restricted to the oceans.

Soil is an important reservoir of fresh water. It transforms discontinuous precipitation into continuous discharges, streams and rivers, and continuously provides moisture to the roots of plants. The rainwater-retention capacity of the soil equals one-third of all fresh water in lakes and reservoirs, and is larger than the volume of riverbeds. Soil water plus ground water are two orders of magnitude greater than all surface fresh water.

Ultimately, all studies in soil hydrology have a single objective: better understanding and fuller description of hydrological processes. The elementary components, infiltration, redistribution, drainage, evaporation and evapotranspiration, are first analysed individually and subsequently considered in combination for a particular sequence of events or season. Also, transport of solutes is considered an integral aspect. A thorough understanding of these processes requires their study at several levels of approximation. One level considers the characterisation and quantification of processes for real soils, i.e. field soils, often called "point-scale" studies (Kutilek and Nielsen, 1994). Such studies require detailed characterisation of the three chief components of the porous soil system: the solid, liquid and gaseous phases.

The solid phase is represented by particles that vary from soil to soil in quality, size and arrangement. In terms of quality, there are two groupings: organic and mineral. Organic matter can be fresh, partially decomposed or decomposed into humus. The composition of the mineral component depends on the parent rock from which the soil formed. Major components are SiO_4, Al_2O_3, Fe_2O_3, CaO, MgO, K_2O, and P_2O_5. Many constituents supply elements essential for plant growth and development, and most of the ninety-two naturally occurring elements can be found in soil.

Particle size is evaluated by mechanical analysis, with three main groupings commonly delineated: sand (0.05–2 mm), silt (0.002–0.05 mm) and clay (<0.002 mm). The relative content of these fractions defines the texture used to classify soils, e.g. silt-loam, clay-loam, sandy-clay. The arrangement of the particles defines structure, and packing of solid material defines the space that is occupied by water or air. An important soil attribute related to the solid phase is bulk density, i.e. the mass of solid material contained per unit bulk volume. Bulk density is inversely related to soil porosity and, therefore, is a factor in compaction and aeration problems.

The liquid phase is a dilute aqueous solution containing a variety of ions, salts and molecules including organic compounds. It represents the pool of nutrients essential for plant growth and development, which is continuously renewed by physical-chemical interactions between soil particles, water and gases. The liquid phase is quantified as soil-water content, which is the mass or volume of water per unit mass of dry soil or per unit volume of bulk soil. In a soil profile, moisture content integrated with depth represents the so-called water storage.

The amount of water in soil is influenced by prevailing conditions. The reservoir is replenished by rainfall, irrigation, and melting snow, and is depleted by evaporation, transpiration, and drainage to deeper zones. For agronomic purposes, a useful range of soil-

water content is defined as available moisture that can be used by plants and is of extreme importance for crop production. In cases of low water availability, irrigation may complement crop needs, and, in cases of excess, drainage facilities may eliminate the surplus.

Organisms in the soil, including plant roots, require a supply of oxygen. Soil aeration depends on the porous space and the degree to which it is occupied by water. An ideal soil is 50% solids, 25% water and 25% air.

The authors' intention is not to provide comprehensive coverage of the processes that occur in soil; detailed textbooks and related journal articles are already available. The present text is restricted to the description of two nuclear techniques, suitable for "point-scale" studies and for porous soil-system characterisation: neutron moderation and γ-radiation attenuation methods, for the measurement of soil-water content and soil bulk density.

1.1. Soil-water content and bulk density

Water content, although a simple concept in soil physics, is difficult to evaluate in the field. Estimates obtained through the many methods available often deviate considerably from the "true" value, which, in reality, is never known. The main problem lies in sampling procedures. Once a soil sample is taken from the field to the laboratory, its water content can be estimated with a high degree of precision and accuracy. However, it is never known if the collected sample truly represents the soil at the desired depth, due mainly to soil variability and uncertainty associated with sampling.

Moisture content can be estimated on a weight or a volume basis. In this work we will use the following symbols and definitions:

– Soil-water content by weight w [(g H_2O) (g dry soil)$^{-1}$]

$$w = \frac{\text{mass of water}}{\text{mass of dry soil}} = \frac{m_w - m_d}{m_d} \tag{1}$$

where

m_w and m_d are the masses of wet and dry soil, respectively (g).

– Soil-water content by volume θ [(cm^3 H_2O)(cm^3 dry soil)$^{-1}$]

$$\theta = \frac{\text{volume of water}}{\text{bulk volume of soil}} = \frac{m_w - m_d}{V} \tag{2}$$

where

V is the volume of the soil sample (cm^3).

In this definition, it is assumed that the density of water is 1 g/cm^3, therefore, (m_w – m_d) is equal to the volume of water. It can be shown that

$$\theta = w \times d_b \tag{3}$$

where

d_b is the bulk density of the dry soil [(g dry soil)(cm^3 of bulk soil)$^{-1}$] defined by

$$d_b = \frac{m_d}{V} \tag{4}$$

Example: In a soil profile, a sample was collected at 20 cm with a volumetric cylinder of 200 cm^3 and 105.3 g. After handling the sample in the laboratory, removing excess soil from the outside of the cylinder and ensuring that the soil occupied the volume V of the cylinder, the sample weighed 395.6 g. After the sample was dried in a ventilated oven at 105^{o}C to a constant weight, its final mass was 335.7 g. In this case,

$$w = \frac{395.6 - 335.7}{335.7 - 105.3} = 0.260 \text{ g g}^{-1} \text{ or } 26\% \text{ by weight}$$

$$\theta = \frac{395.6 - 335.7}{1 \times 200} = 0.300 \text{ cm}^3 \text{ cm}^{-3} \text{ or } 30\% \text{ by volume}$$

$$d_b = \frac{335.7 - 105.3}{1 \times 200} = 1.152 \text{ g cm}^{-3}$$

and, according to eq. (3),

$$0.300 = 1.152 \text{ [(g dry soil)(cm}^3 \text{ of bulk soil)}^{-1}] \times 0.260[(\text{g } H_2O)(\text{g dry soil})^{-1}]$$

The several methods for determining soil-water content and bulk density differ mainly in terms of sampling method, but equations (1) through (4) are always applicable when the information is available. The greatest difficulty lies in the measurement of V, because sampling with a simple auger destroys the structure of the soil. In this text we will not discuss the "classical" methods of soil-water measurement, which are covered in basic soil physics texts, such as the Methods of Soil Analysis monograph (Klute,1986).

A disadvantage of the classical methods is their destructive feature. With each sampling event, the soil profile is disturbed. Even with a simple auger, several samplings will destroy a small plot. Soil variability presents an additional problem; collecting soil at the "same" depth requires another location to be sampled. A third problem, albeit minor, is the time required for oven-drying each sample. The minimum is 24 h.

With the use of a neutron probe, which we will discuss in detail, there is little disturbance of the soil profile. Only once is it necessary to introduce an access tube to a desired soil depth, and, thereafter, measurements can be taken repeatedly at any depth or time, in a matter of minutes. Of course, there are disadvantages with the neutron probe, which will be discussed also.

2. DEPTH NEUTRON PROBES

2.1. Instrument description and working principles

A neutron probe consists of two main parts: the probe and shield, and the electronic counting system. In some models these parts are separable.

2.1.1. The probe and shield

The probe is a sealed metallic cylinder 3 to 5 cm in diameter and 20 to 30 cm in length. It contains a radioactive source that emits fast neutrons, a slow neutron detector, and a pre-amplifier. The signal from the pre-amplifier passes through a 5- to 20-m long cable to the electronic counting system.

The geometry of the probe, type and activity of the neutron source, type of detector and pre-amplifier vary considerably depending on manufacturer. Neutron sources are a mixture of an alpha-particle emitter (e.g. americium and radium) and a fine powder of beryllium. When alpha particles bombard beryllium nuclei:

$$ {}^{4}_{2}\alpha + {}^{9}_{4}Be \rightarrow {}^{1}_{0}n + {}^{12}_{6}C $$

The neutrons have energies up to 14 MeV, (1 eV = 1.6×10^{-19} J), with an average value of approximately 4.5 MeV (fast neutrons).

The strength of the source is generally given by the activity of the alpha emitter, in becquerels (Bq). Most sources have an activity in the range of 370 to 1,850 MBq (10–50 mCi). Most alpha emitters also emit γ radiation and fast neutrons. Therefore, protection of the user is an important issue. The shield, which is the container for the probe, has to be properly designed to provide such protection. Commercially manufactured probes stored in a shield expose the user only to permissible levels of radiation.

The user is exposed to γ radiation and fast neutrons if the probe is not in the protective shield. *Such exposure should be absolutely avoided.* The design of the shield and probe allows the probe to leave the shield and pass immediately into the soil, avoiding excessive radiation exposure.

Shielding from γ radiation is most efficiently provided by lead, whereas shielding from fast neutrons is provided by paraffin, polyethylene, or other material high in hydrogen content. Hence, neutron-probe shields are generally made of lead and a hydrogen-containing material.

During measurements, the probe is lowered to the desired depth in the soil inside an aluminium access tube that is “transparent” to fast neutrons, which are scattered by the soil within 30 to 50 cm of the source. As a result of this scattering, the neutrons lose energy and are slowed. This interaction is used to estimate moisture content, as described below.

Close to the source is a detector that counts only slow, not fast, neutrons. Several slow-neutron detectors are available, e.g. $^{10}BFl_3$, ^{3}He, and scintillation detectors, each of which has advantages and disadvantages.

The pulses from the detector are first pre-amplified within the probe. Only these pre-amplified pulses are sent to the electronic counting system through the cable that connects the two parts of the instrument.

2.1.2. Electronic counting system

Although electronic counting systems vary according to probe type, all comprise an amplifier, a high-voltage source, a counter, a timer, rechargeable batteries and a microprocessor. Inasmuch as neutron emission is a random process (following Poison's Law), counting time strongly influences the statistical accuracy of estimating the soil-water content, therefore most probes offer several counting options. With each count corresponding to an impulse originating from one slow neutron reaching the detector, the microprocessor converts the raw count data into counts per minute (cpm) or per second (cps).

Present day neutron probes have microprocessors that utilise calibration equations supplied by the maker, or developed by the user, for several soils, and the results are given directly in soil-water content (%, g g^{-1}, cm^3 cm^{-3}) for each depth and location, or in terms of water stored in a given soil layer [(mm H_2O)(10 cm of soil)$^{-1}$] or profile.

Because each manufacturer provides operational instructions, such details will not be discussed here. Figure 1 is a schematic diagram of a depth neutron probe being used in the field to measure soil-water content at a particular depth.

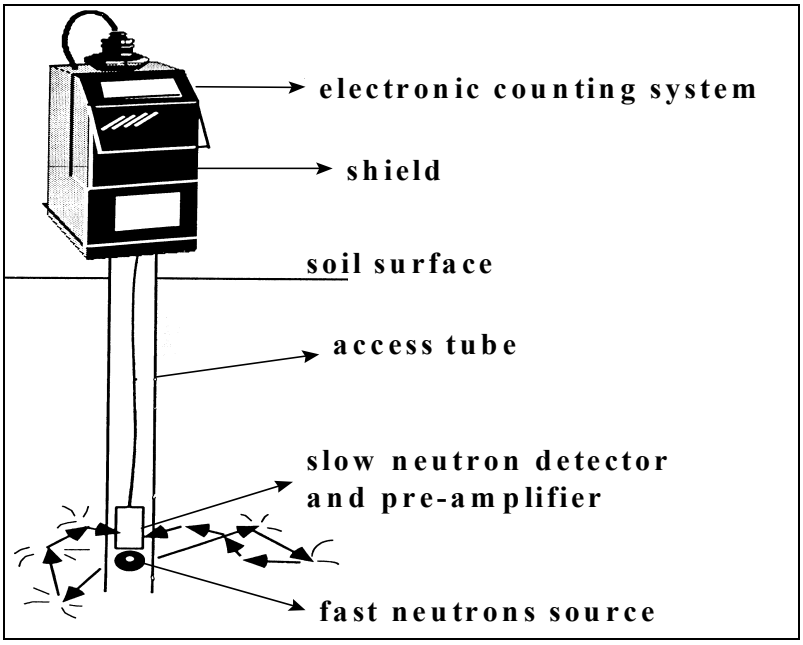

FIG. 1. Depth neutron probe in working position.
(Source: Campbell Pacific Nuclear (CPN®), 503 DR Hydroprobe Operating Manual)

The working principle is straightforward. The neutron source emits fast neutrons that interact with particles and water that surround the probe. Since neutrons have no charge, the electric fields associated with charged soil particles do not affect their movement. Three processes occur during this interaction: neutron absorption by nuclei, neutron scattering through collisions, and neutron disintegration.

Neutron absorption by nuclei depends on the energy of the neutron and the particular target nucleus. The "probability" of this process is measured through the cross section of the reaction, which, in general for most of the elements present in soil, is very low. If the reaction occurs, one neutron is absorbed by a nucleus ${}^{A}_{Z}X$, according to

$${}^{1}_{0}n + {}^{A}_{Z}X \rightarrow {}^{A+1}_{Z}X$$

where

${}^{A+1}_{Z}X$ is the new nucleus.

In some cases, the new nucleus is unstable and disintegrates emitting radiation. This is the same principle as neutron activation, and occurs only with a few nuclei in soil, e.g. Ag, Au, In, Fe, Al, Mn, which are present usually in very low concentrations. Also, because the neutron flux generally has a very low intensity, the probability of a neutron capture is extremely low. In many cases ${}^{A+1}_{Z}X$ is stable (e.g. ${}^{12}_{6}C + {}^{1}_{0}n \rightarrow {}^{13}_{6}C$; ${}^{14}_{7}N + {}^{1}_{0}n \rightarrow {}^{15}_{7}N$), and, when radioactive, half-lives are generally very short (e.g. ${}^{23}_{13}Al + {}^{1}_{0}n \rightarrow {}^{24}_{13}Al$ with a half-life of 2.3 min). Therefore, there is virtually no activation of soil material by the neutron probes here described. Moreover, if the aluminium access tube becomes slightly radioactive during use, decay occurs in only a few minutes.

Neutron scattering by elastic and non-elastic collisions is the most important process on which the working principle of the neutron probe is based. Through collisions, fast neutrons (high energy, >2 MeV) lose energy (moderation) and become slow or thermal neutrons (low energy, <0.025 eV). As illustrated in Table I, if collisions are elastic, the heavier the target nucleus the less energy is lost by the neutron.

TABLE I. NUMBER OF ELASTIC COLLISIONS NECESSARY TO REDUCE THE ENERGY OF A NEUTRON FROM 2 MeV TO 0.025 eV

Target isotope	Collisions
^{1}H	18
^{2}H	25
^{4}He	43
^{7}Li	68
^{12}C	115
^{16}O	152
^{238}U	2,172

Because ^{1}H is the target atom that most efficiently reduces neutron energy, hydrogen is said to be a good neutron moderator. Because of its hydrogen content, water is a good neutron moderator, hence, the wetter the soil, the greater the number of slow neutrons in the presence of a fast-neutron source. With the exception of organic matter, which may gradually change with time, soil materials containing hydrogen remain constant and are taken into account during calibration.

Free neutrons are unstable and disintegrate with a half-life of 13 min. Hence, if a free neutron is not captured it disintegrates according to

$${}^{1}_{0}n \rightarrow {}^{1}_{1}p + \beta^{-} + \nu + 780 \text{ keV}$$

where

${}^{1}_{1}p$ is a proton, β^{-} is a beta particle, and ν is a neutrino.

When the probe is lowered into the access tube, a stable, spherical "cloud" of slow neutrons develops quickly around the source, with a diameter of about 30 cm. The drier the soil, the greater is the diameter of the cloud. The number of slow neutrons per unit volume at each point of the cloud remains constant and is proportional to the water content of the soil within the cloud. Since the slow neutron detector is placed inside the cloud volume, the count rate (cpm or cps) is proportional to the soil-water content, θ, of the same volume. The instrument is calibrated with samples of known θ measured by the gravimetric method. Calibrations details are provided in Section 2.4. More information on neutron-moisture-meter theory is available in the literature (IAEA, 1970; Greacen, 1981).

2.2. Radiation protection and safety of neutron and gamma probes

2.2.1. Occupational exposure and radiation protection

Occupational exposure to radiation can occur as a result of various human activities, including the use of radioactive sources in industry, agriculture, medicine and many fields of research, and occupations that involve the handling of materials with enhanced concentrations of naturally occurring radionuclides. Adequate radiation protection of the workers is essential for the safe and acceptable use of radiation, radioactive substances and nuclear energy.

In 1996, the International Atomic Energy Agency published basic safety standards, or **BSS**: "International Basic Safety Standards for Protection Against Ionising Radiation and for the Safety of Radiation Sources" (IAEA Safety Series No. 115) and "Radiation Protection and the Safety of Radiation Sources" (IAEA Safety Series No. 120). These were sponsored jointly by the Food and Agriculture Organization of the United Nations (FAO), the IAEA, the International Labour Organization (ILO), the Organization for Economic Co-operation and Development Nuclear Energy Agency, the Pan American Health Organization, and the World Health Organization. They set out the objectives and principles for radiation safety and the requirements to be met to apply the principles and to achieve the objectives (FAO et al., 1996a; FAO et al., 1996b).

Guidance on meeting the basic safety standards for occupational radiation protection is provided in the IAEA Safety Guides, which are published jointly by the IAEA and the International Labour Office. IAEA Safety Guide No. RS-G-1.1 provides general guidance on the establishment of effective radiation protection programmes for occupational exposure (IAEA and ILO, 1999). These safety standards are not legally binding on Member States, but may be used by them, at their discretion, to draw up national regulations with respect to their own activities. Governments, however, have responsibility for enforcement, generally through the establishment of a federal system responsible for radiation protection and safety. Such national infrastructure includes: legislation and regulations; a regulatory authority empowered to authorise and inspect regulated activities and to enforce the legislation and regulations; sufficient resources and adequate numbers of trained personnel (IAEA and ILO, 1999).

In this section, only basic aspects related to radiation protection and safety are covered. In addition, the user should always consider specific national legislation and regulations.

2.2.2. Basic concepts of radiation physics

2.2.2.1. Nuclear reactions and radioactivity

The atomic nucleus is composed of positively charged protons and neutral neutrons that interact as various forces: electrical, gravitational, and nuclear. The equilibrium of these forces depends on the numbers of protons (Z = atomic number) and neutrons (N), present in the nucleus, and defines the condition of nuclear stability. This proportion defining the stability of a nucleus is not constant for all atoms, and depends on the mass number ($A = Z + N$) according to the empirical relation

$$Z = \frac{A}{2 + 0.0146\ A^{2/3}}$$

Hence, a given atom may be unstable or radioactive due to an excess of protons (Z much larger than N) or due to an excess of neutrons (N much larger than Z), presenting a natural tendency for the establishment of equilibrium through different types of transformations. Here, we present two examples related to neutron probes: a mixture of americium and beryllium isotopes as a source of neutrons, and an isotope of caesium as a source of γ rays.

Americium, an unstable isotope with an excess of protons (Z/N = 95/146 = 0.65), tends toward equilibrium by emitting an alpha particle of energy 5.48 MeV and a γ ray of 60 keV, according to

$$^{241}_{95}Am \rightarrow {}^{237}_{93}Np + {}^{4}_{2}\alpha + E$$

Compared to americium, the resulting isotope of neptunium has less of an excess of protons with the smaller Z/N ratio, 0.64. Neptunium is also unstable and subsequent transformations occur until equilibrium is reached.

Beryllium, the other constituent of the mixture, contains an excess of neutrons (Z/N = 0.8) and reacts with the alpha particle emitted from the americium,

$$^{9}_{4}Be + {}^{4}_{2}\alpha \rightarrow {}^{12}_{6}C + {}^{1}_{0}n + E$$

Compared to $^{9}_{4}Be$, the new isotope $^{12}_{6}C$ has less of an excess of neutrons with the higher Z/N ratio, 1.

The unstable isotope $^{137}_{55}Cs$, with an excess of neutrons (Z/N = 0.67), transforms as

$$^{137}_{55}Cs \rightarrow {}^{137}_{56}Ba \rightarrow {}^{137}_{56}Ba + \beta^{-} + \gamma(661.6\ \text{keV})$$

In this reaction, the stable isotope of barium is produced either by the emission of a β^- particle having an energy of 1,176 keV or mainly by the emission of a β^- particle with an energy of 514 keV followed by an emission of γ radiation of 661.7 keV.

If a probe contains both neutron and γ ray sources, it is understood from the above reactions that four types of radiation are emitted: α, β, γ, and neutrons.

2.2.2.2. Definitions and units

The main physical quantities are the **activity** or rate of nuclear transformation of radionuclides and the **absorbed dose** or energy absorbed by a unit mass of a substance from the radiation to which it is exposed. The unity of activity is the reciprocal second, representing the number of nuclear transformations (or disintegrations) per second, or **becquerels** (Bq). The previously used unit of activity was the curie, which is equivalent to 3.7×10^{10} Bq. The unit of absorbed dose, the joule per kilogram, termed **gray** (Gy), is the basic physical dosimetric quantity of the BSS. However, this is not entirely satisfactory for radiation purposes because the degree of damage to human tissue differs with the type of ionising radiation. Consequently, the absorbed dose, averaged over a tissue or organ is multiplied by a radiation-weighting factor (w_R) to take account of the effectiveness of a given type of radiation in inducing health effects; the resulting quantity is termed the **equivalent dose**. The likelihood of injurious stochastic effects due to a given equivalent dose depends on the type of organ or tissue. Consequently, the equivalent dose to each organ or tissue is multiplied by a tissue-weighting factor that takes account of the radiosensitivity. The sum of such weighted equivalent doses for all exposed tissues in an individual is termed the **effective dose**. The unit of equivalent dose and of effective dose is the same as for absorbed dose, namely joule per kilogram, but the name **sievert** (Sv) is used to avoid confusion with the unit for absorbed dose (Gy) (FAO et al., 1996a).

2.2.2.3. Biological effects of radiation

Exposure to radiation, including to neutrons at high doses, may have effects such as nausea, reddening of the skin, or, in severe cases, more acute syndromes that are clinically expressed within a short period of time. Such effects are termed “deterministic” because they are certain to occur if the dose exceeds a threshold level. Radiation exposure also may have somatic effects such as malignancies, which are expressed after a latency period and may be epidemiologically detectable in a population; this induction is assumed to take place over the entire range of doses, without a threshold level. Also, hereditary effects, due to radiation exposure have been statistically detected in non-human mammalian populations, and are presumed to occur in human populations. These epidemiologically detectable malignancy and hereditary effects are termed “stochastic” because of their random nature.

Deterministic effects are the result of various processes, mainly cell death and delayed cell division, caused by exposure to high levels of radiation. The severity of a particular deterministic effect in an exposed individual increases with the dose above a threshold for the occurrence of the effect.

Stochastic effects may ensue if an irradiated cell is modified rather than killed. Modified cells may, after a prolonged process, develop into cancer. If the damage is to a germ cell, the function of which is to transmit genetic information to progeny, hereditary effects of various types may develop in the descendants of the exposed individual. The likelihood of stochastic effects is presumed to be proportional to the dose received, without a dose threshold. The probability of occurrence of a stochastic effect is higher for higher doses, but the severity that may result from irradiation is dependent on the dose (FAO et al., 1996a).

2.2.3. Basic safety standards for radiation protection and safety of sources

Human activities that add radiation to the exposure that is normally incurred from background radiation, or that increase the likelihood of their incurring exposure, are termed "practices" in the BSS, e.g. use of neutron and gamma probes. Human activities that seek to reduce existing radiation exposure, or the likelihood of incurring exposure that is not part of a controlled practice, are termed "interventions" (FAO et al., 1996a).

In order to keep doses from practices below regulatory limits and as low as reasonably achievable (ALARA minimisation principles), there is a series of basic safety requirements to be adhered to. For convenience, they have been grouped into administrative requirements (authorisation, responsibilities of registrants and licensees), radiation protection requirements (justification of practices, dose limitation, optimisation of protection and safety, dose constraints), management requirements (safety culture, quality assurance, control of human factors), technical requirements (security of sources, defence in depth, good engineering practices), and verification of safety (safety assessments, monitoring and verification of compliance, records) (FAO et al., 1996a; IAEA and ILO, 1999; Oresegun, 2000).

The National Regulatory Authority is responsible for all aspects of radiation protection and safety in a country. Its general functions include the following: the assessment of applications for permission to conduct practices that entail or could entail exposure to radiation; the authorisation of such practices and of the sources associated with them, subject to certain specified conditions; the conduct of periodic inspections to verify compliance with the conditions; and the enforcement of any necessary actions to ensure compliance with the regulations and standards (FAO et al., 1996a; IAEA and ILO, 1999).

2.2.4. Operational radiation safety

In order to achieve operational radiation safety, there must be compliance with the safety requirements as indicated by the IAEA's BSS, and specified by the National Regulatory Authority of each country. In practical terms, regarding the use of neutron and gamma probes, the following components should be considered: design and manufacture; training; operational instructions; local rules; transport safety; personnel monitoring and dosimetry; safe storage and disposal; maintenance; emergency preparedness; inventory, accountability and record keeping. With regard to the latter, the following records must be kept: i) inventory of sources and accountability, ii) personnel monitoring doses, iii) training and retraining of workers, iv) maintenance and repair of equipment, v) results of leak tests, vi) log book of calibration and use of survey/dose rate meters, vii) log book of off-site locations, viii) transportation documentation, ix) audits and review of the radiation safety programme, x) incidents and accidents investigation records (FAO et al., 1996a; IAEA and ILO, 1999; Oresegun, 2000).

2.2.5. Occupational exposure and dose limitations

As mentioned in Section 2.2.2.2., for radiation purposes it is necessary to consider a radiation-weighting factor (w_R) for the absorbed dose, to account for the relative severity of various types of radiation in inducing health effects. The multipliers are shown in Table II for the four types of radiation associated with neutron and gamma probes. During handling of such probes, the neutrons and γ radiation are of chief concern, the α- and β-radiation being sufficiently attenuated by the metal capsule sealing the two sources (FAO et al., 1996a).

TABLE II. CHARACTERISTICS OF THE FOUR TYPES OF RADIATION

Type	Mass	Charge	Radiation weighting factor (w_R)
α	4	+2	20
β	0.0006	–1	1
Neutrons	1	0	
<10 keV			5
10 to 100 keV			10
100 keVto 2 MeV			20
2 to 20 MeV			10
>20 MeV			5
γ	0	0	1

Because neutrons have no charge, their penetration power is high. They can pass completely through the human body. During such penetration, they transmit all or part of their kinetic energy, damaging tissues and organs. Because of this penetration power, the w_R values vary from 5 to 20 according to the neutrons' energies. This means that for similar absorbed doses, damage to the human body from neutrons is five- to twenty-fold greater than that from γ radiation. Neutron-probe shields are manufactured from synthetic materials rich in hydrogen that efficiently attenuate neutrons; operator exposure is thus confined to acceptable levels. In the case of gamma probes, γ radiation is efficiently shielded by lead, thus posing a problem for manufacturing portable gamma probes.

The main concern is radiation escape from the soil while making measurements, especially under dry conditions and when the radius of influence is large. With the good practices outlined above, as well as good design and manufacture of gauges, the occupational doses recorded in the industry have been well below annual dose limits. Applying ALARA principles, such as the use of Teflon plastic reflectors laid on the surface, doses as low as 0.2 mSv yr^{-1} (1% of the annual dose limit) have been reported for neutrons and γ rays (Guzmàn, 1989).

2.2.5.1. Occupational dose limitations

A **dose limit** is defined in the BSS as "the value of the effective dose or the equivalent dose to individuals from controlled practices that shall not be exceeded" (FAO et al., 1996a).

The occupational exposure of any worker shall be so controlled that the following dose limits are not exceeded:

a) an effective dose of 20 mSv per year averaged over 5 consecutive years,
b) an effective dose of 50 mSv in any single year,
c) an equivalent dose to the lens of the eye of 150 mSv in a year, and
d) an equivalent dose to the extremities (hands and feet) or to the skin of 500 mSv in a year.

For a person aged 16 to 18 years, the occupational dose limits should be the following:

a) an effective dose of 6 mSv per year,
b) an equivalent dose to the lens of the eye of 50 mSv in a year, and
c) an equivalent dose to the extremities or the skin of 150 mSv in a year.

For members of the public, estimated annual doses should not exceed:

a) an effective dose of 1 mSv in a year,
b) in special circumstances, an effective dose of up to 5 mSv in a single year provided that the average dose over 5 consecutive years does not exceed 1 mSv per year,
c) an equivalent dose to the lens of the eye of 15 mSv in a year, and
d) an equivalent dose to the skin of 50 mSv in a year.

The IAEA is planning to publish a radiation safety guide for nuclear gauges. Normal and potential exposures will both be covered.

With regard to radiation safety, it may be concluded from the above that the use of neutron probes poses not only acceptable health and safety risks, but, in fact, negligible risks. The use of neutron gauges is not, and should not, be classified as a practice of high potential hazard to human health.

2.3. Access tubes and their installation

Size and type of access tube depend on the diameter of the probe as well as cost and availability of tubing. Unfortunately, probe diameter has not been standardised internationally.

The best access-tubing material is aluminium because it is transparent to neutrons and resists corrosion. Other materials that are used (steel, iron and brass as well as polyethylene and other plastics), differ with respect to neutron interaction. Once a particular kind of tubing is chosen, calibration and all experimental work must be done with the same material. Steel and brass slightly affect probe sensitivity owing to absorption of neutrons by iron and copper. Count rates are increased by the hydrogen in polyethylene and other plastic tubes.

Normally, the manufacturer specifies the inside and outside diameters of the tubing. An air gap between the probe and the tube wall reduces sensitivity, therefore, the inside diameter should be just large enough for the probe to move freely without friction.

Tube length depends on the greatest depth at which measurements will be made. It should always be 10 to 20 cm more than the greatest measurement depth to allow the active centre of the probe to be placed at the optimum depth. Also, the tube should extend 20 to 40 cm above the soil in order to facilitate positioning the shield case on top. Each tube should be fitted with a rubber stopper, or covered with an inverted aluminium can, to exclude water and debris. The bottom of each tube should be sealed with a rubber stopper or other material to exclude water from a shallow water table. When the deepest measurements are above the water table, no stopper is necessary.

Although there are several methods for installing access tubes (Greacen, 1981), each requires that a hole be made to the appropriate depth. The primary purpose of each method is to avoid air gaps between soil and tube, which is often achieved by using an auger with a diameter slightly smaller than that of the outside of the access tube. After augering to the

desired depth, the access tube is driven into the hole, often with difficulty, and some soil from the wall of the hole enters the tube. This soil is removed with a second auger of a diameter slightly smaller than that of the inside of the tube. Alternatively, the tube may be driven directly into the soil in increments of about 20 cm, after each of which soil inside the tube is removed with an auger, as above. Care must be taken to remove all of the soil inside the tube. A third procedure would be to introduce a guide tube of the same diameter as the access tube to the desired depth, and then remove it for placement of the access tube.

With stony, heavy-swelling, and layered soils, the installation of access tubes may be extremely difficult. In such cases, the researcher must rely on experience and use ingenuity. It should be remembered that the installation of an access tube is done only once for a given experiment, therefore, it must be done with care, even if it takes great effort over several hours. An improperly installed access tube will compromise all measurements made thereafter. It should be remembered also that an advantage of the neutron-moderation method is that the disturbance of the soil occurs only during tube installation and, thereafter, rapid measurements can be made over long periods, always sampling the same location in the field. More information on access-tube installation is available elsewhere (IAEA, 1976).

2.4. Calibration

The calibration of a neutron probe consists of quantifying the relationship between probe output in cpm and soil-water content θ [(cm^3 of H_2O)(cm^3 of bulk soil)$^{-1}$]. Samples of a given soil, with a wide range in water content, are used to generate cpm data with the probe and θ values are determined by classical methods. It is a simple procedure in theory, but can be difficult and tedious depending on the properties of the soil profile and the chosen experimental design. First, we will discuss making a calibration curve for one depth of a homogeneous soil, and then extend the discussion to consider more difficult situations.

Sampling is the main problem in calibration. Theoretically, the soil exposed to the neutron probe to obtain cpm should be sampled to measure θ. However, the neutron method monitors an ill-defined large volume, assumed to be a sphere of 30-cm diameter, whereas classical soil-moisture-determination methods use much smaller samples. This disparity is minimised by taking several samples to determine θ around the access tube near the position of the probe at which the cpm data are obtained. In most cases, there is no guarantee that both methods sample the same volume of soil, and the problem is worse with heterogeneous, layered or stony soils.

Obtaining a wide range of water contents for a soil is another practical problem. Although it is possible through wetting (irrigation or rainfall) and drying (evaporation or drainage), it requires tedious operations for long periods of time over several locations. Because a soil does not wet or dry uniformly throughout its profile, the water content inferred by the neutron probe is a spatial average for an unknown volume. Hence, both the position and volume of actual soil sampled remain somewhat uncertain.

Having achieved the best possible set of data, we construct a calibration graph from pairs of data (cpm, θ). First, in order to avoid electronic drift from temperature and other factors that affect the probe, we do not use cpm obtained directly, but use the count ratio CR, which is defined as

$$CR = \frac{\text{count rate in soil}}{\text{count rate in standard}} = \frac{N}{N_s} = \frac{C \times T^{-1}}{C_s \times T_s^{-1}} \quad (5)$$

where

C is count measured in the soil during time T (min),
C_s is the count measured in a standard material during time T_s (min),
N is the count rate in the soil (cpm),
and N_s is the count rate in the standard material (cpm).

Table III shows field data obtained during calibration of a probe at 20-cm depth. Each time the neutron probe is used, it should be checked for stability by taking readings in a standard material, which, in most cases is inside its protection shield, sitting on the probe transportation case to maintain standard conditions. When water is the standard material, the access tube, sealed at its base is placed in the middle of a large container of water.

TABLE III. CALIBRATION DATA FOR A PROBE WITH A NEUTRON SOURCE OF 1,480 MBq (40 mCi) Am/Be IN AN ALFISOL AT PIRACICABA, BRAZIL

Pairs	θ (cm^3 cm^{-3})	N (cpm)	CR[a]
1	0.424	79,650	0.507
2	0.413	75,541	0.481
3	0.393	76,169	0.485
4	0.387	71,143	0.453
5	0.378	67,846	0.432
6	0.375	69,259	0.441
7	0.306	59,208	0.377
8	0.287	57,637	0.367
9	0.291	62,035	0.395
10	0.283	58,109	0.370

[a]Determined as in eq. (5). N_s in water = 157,050 cpm.

C_s is the standard count rate, N_s, in water, which should be constant over long periods of time, fluctuating only within statistical deviations normally taken as $\pm\sqrt{C_S}$ (Poisson's distribution). Each manufacturer gives details of these procedures for their probes.

Figure 2 shows the graph of θ versus CR. It follows the linear equation obtained through classical linear regression $y = a + bx$, $\theta = -0.095 + 1.04 \times CR$

With CR taken as the independent variable and θ as the dependent variable, the linear regression coefficient $R = 0.966$.

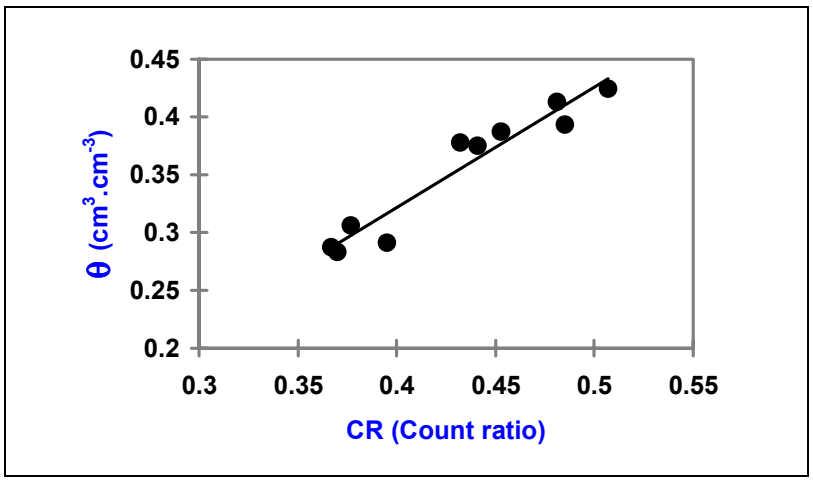

FIG. 2. Calibration equation obtained with Table-III data.

As will be shown later, variances of the intercept *a* (–0.095) and of the slope *b* (1.04), and their covariance contribute to the calibration error. Because these variances are the primary errors in the use of neutron probes, they must be minimised. In general, the closer the value of *R* is to unity, the smaller are these variances. Provided the relationship is truly linear, values of *R* close to unity can be achieved by increasing the number of pairs of observations (cpm, θ) and expanding the range of soil-water contents measured, including data generated with very wet (close to or at saturation) and very dry samples.

The intercept of the calibration curve varies from soil to soil and probe to probe. It should not be zero nor close to it since it is an extrapolated value out of the calibration range. Although no theoretical significance is assigned to the intercept, it is related to the hydrogen content of the soil; a dry soil high in hydrogen presents a higher intercept.

The slope of the calibration varies also from soil to soil and probe to probe. Being the derivative of the calibration line, it represents the **sensitivity** of the probe. It is the change in soil-water content per unit change in count ratio. Within certain limits, the smaller its value, the more sensitive is the probe. In other words, for small changes in soil-water content (the variable desired), there are large changes in count ratio (the variable measured).

Because of neutron interactions in the soil, geometry of the probe, type of neutron detector, electronics, etc., a different calibration line is obtained for each soil with a given neutron probe. Soil characteristics–mainly chemical composition and bulk density–also affect the calibration line (Grimaldi et al., 1994). Therefore, for a specific soil, calibration lines are related to soil bulk densities d_b (Fig. 3). In general, the calibration lines are parallel for different bulk densities of the same soil. For extremely layered soils, especially those with layers of different composition, e.g. some alluvial soils, slopes differ for each layer.

In addition to the difficulty of installing access tubes, the definition of θ is also a special problem for gravely and stony soils. Some authors define θ using the bulk volume for the total sample volume including that occupied by gravel, whereas others exclude the volume occupied by gravel. Each gravely soil is unique, therefore the neutron probe user must explore the best means of obtaining useful calibration curves. Whether it is necessary to generate different calibration curves for slightly different soils or for slightly different bulk densities will depend on the objectives of the experiment. The accuracy needed for the determination of θ is the most important criterion.

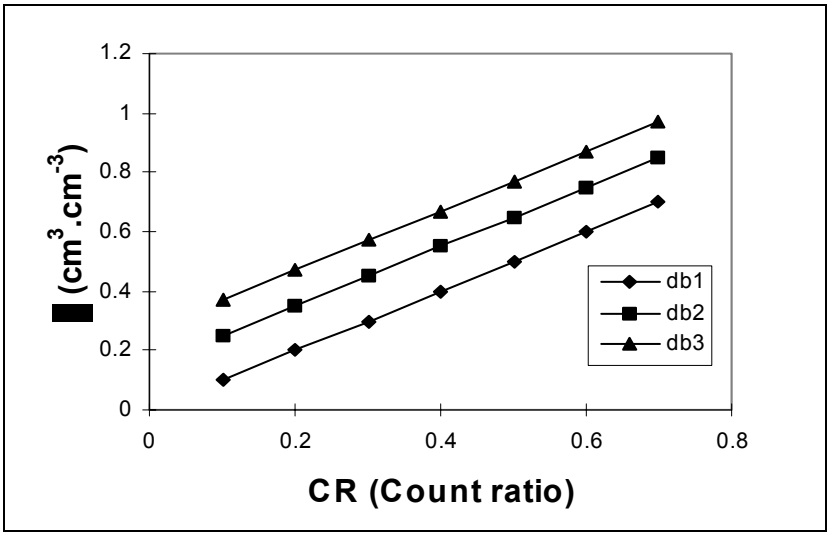

FIG. 3. Theoretical calibration lines for soil bulk densities $d_{b1} > d_{b2} > d_{b3}$.

2.4.1. Laboratory calibration

Laboratory calibration involves the use of packed soil samples with discrete levels of soil-water content, θ, and soil bulk density, d_b. Usually, large amounts of soil are packed into drums of 80- to 120-cm diameter and 80- to 120-cm height. The access tube is placed in the centre. Packing should be done carefully in order to ensure homogeneity of θ and d_b–a difficult, laborious task.

Many neutron-probe manufacturers have a collection of such sealed drums representing a wide range in soil-water contents, for calibration of new probes and production of a factory-calibration curve for each probe. Although its use is somewhat limited because it is derived for only one soil or soil material, it is useful to compare the factory calibration to that for a soil being studied by the user. Commonly, because their slopes are nearly identical, the factory-calibration curve can be used when the objective is to measure changes in soil-water content rather than generate absolute values of θ.

2.4.2. Field calibration

Field calibration involves the installation of access tubes, measurements of cpm with the probe, and immediate collection of soil samples at appropriate depths around the access tube to measure θ by classical means. This procedure is repeated using several access tubes at a given time to obtain a desired number of replicated sets of observations of θ and cpm within a soil profile for a given distribution of soil-water contents. The procedure is repeated, when soil varies from very wet to very dry, with more access-tube locations to achieve paired observations of θ and cpm over the entire range of moisture contents to be later monitored in field investigations. Under normal field conditions, it is difficult to obtain such a wide range of soil-moisture levels. To obtain very wet conditions, irrigation is likely to be required. Dry conditions can be difficult to obtain, especially in humid and sub-humid regions. Even in arid regions with water being extracted by plant roots, the soil-water content may not decrease much below the permanent wilting point except near the surface owing to evaporation. Because soils do not dry uniformly throughout the profile, and may be stratified, the resulting distribution of θ introduces error in the calibration of neutron probes.

2.4.3. Quick field calibration

Carneiro and De Jong (1985) developed a method for quickly obtaining a calibration curve in the field, using a neutron probe to measure changes in count ratio within the soil profile as a result of applying a known amount of irrigation water. The slope, *b*, of the calibration is determined from the equation

$$b = \frac{S_f - S_i}{[\sum_0^z CR_f \times \Delta z - \sum_0^z CR_i \times \Delta z]} \tag{6}$$

where

S_f is the final soil-water storage [see eq. (35)] calculated from the surface to the water-penetration depth z (mm) into the soil profile,
S_i is the initial soil water storage to depth z (mm),
and CR_f and CR_i are the final and initial count ratios corresponding to depth increases Δz, respectively.

Because the change in soil-water storage corresponds to the applied irrigation water depth, the difference $(S_f - S_i)$ is known, hence b of the neutron calibration curve is known. The value of a is calculated from

$$a = \theta - b \times CR \tag{7}$$

with the value of θ obtained from a soil sample taken from the field at the time CR is measured with the neutron probe. The soil sample is analysed gravimetrically in the laboratory.

Example: Before and after the application of 150 mm of water to a soil, the following count rates were obtained.

Depth (cm)	CR_i	$CR_i \times \Delta z$	CR_f	$CR_f \times \Delta z$
0–30	0.22	6.6	0.55	16.5
30–60	0.35	10.5	0.58	17.4
60–90	0.32	9.6	0.40	12.0
90–120	0.30	9.0	0.30	9.0
	$\sum_0^{120} CR_i \times \Delta z$	35.7	$\sum_0^{120} CR_f \times \Delta z$	54.9

The slope of the calibration curve is calculated from eq. (6) as

$$b = \frac{S_f - S_i}{[\sum_0^{120} CR_f \times \Delta z - \sum_0^{120} CR_i \times \Delta z]} = \frac{15}{54.9 - 35.7} = 0.781$$

A soil sample taken in another situation at the 30-cm depth had a water content θ = 0.434 cm^3 cm^{-3} determined by the gravimetric method. The corresponding *CR* obtained in the field at the same depth was 0.45. Therefore, with the value of *a*, calculated from eq. (7) as

$$a = \theta - bCR = 0.434 - 0.781 \times 0.45 = 0.0824$$

the final calibration equation becomes

$$\theta = 0.0824 + 0.781 \times CR$$

2.4.4. Theoretical models

Calibration equations have been developed also from theoretical models based on neutron-diffusion theory. One of the most widely accepted models (Couchat et al., 1975) is based on the measurement of neutron absorption and diffusion cross sections in a graphite pile. Soil samples analysed in a specialised laboratory with the graphite pile yield a linear calibration equation as a function of soil moisture and bulk density. Vachaud et al. (1977) presented a systematic study of comparisons between gravimetric and theoretical calibrations.

2.4.5. Calibration for surface layers

The calibration of neutron probes for measuring water content near the soil surface requires special considerations. Many authors do not recommend the utilisation of depth neutron probes for surface determinations, although specially designed neutron probes have been developed for this purpose (Chapter 3).

Several approaches have been used for measuring soil moisture in surface layers. One approach, which takes into account the escape of neutrons to the atmosphere, is to obtain separate calibration curves for individual shallow-depth layers (Greacen, 1981). Another is to use neutron deflector/absorbers made of paraffin or polyethylene. A hole in the centre of thick discs of paraffin or polyethylene allows these deflector/absorbers to be placed on the soil surface immediately around the access tube (Arslan et al., 1997). Although this method provides reliable calibration curves, the deflector/absorbers have proven impractical in many situations for routine measurements. Some believe that it is possible to obtain directly a calibration specific for the surface layer (0–15 cm) by correlating the counting rates with the source at 10-cm depth and the water content of samples taken at 0 to 15 cm (Haverkamp et al., 1984).

2.5. Sphere of influence

The probe "sees" an approximately spherical cloud of slow neutrons, termed the "sphere of influence" or "sphere of importance." Theoretical studies show that the radius is a function of the soil-water content (i.e. the hydrogen content) (IAEA, 1970). In pure water, the radius of the sphere of influence is approximately 5 to 8 cm. In very dry soils it may be 20 cm or more. Olgaard's (1969) theoretical model suggests that, for a value of θ = 0.1 cm^3 cm^{-3}, which is extremely low in agronomic terms, the radius is always less than 45 cm. Because the sphere of influence is not constant even for the same soil and the same instrument, special consideration should be given to the measurement and interpretation of neutron-probe readings both when making a calibration curve and when monitoring soil moisture in the field. This consideration is particularly important for shallow depths in dry soils. Therefore, it is

important to know the diameter of the sphere of influence as a function of θ, thus the probe can be placed just deeply enough to prevent loss of neutrons to the atmosphere.

It is best to measure the radius of the sphere of influence in the laboratory using homogeneous medium such as soil uniformly packed in drums. Measurements can be made also in the field whenever water-content distribution is nearly constant within a fairly homogeneous soil. The experimental procedure is straightforward. The probe is lowered to a depth greater than the maximum value of the radius of influence, R_i., usually to 45–50 cm. After taking an initial count rate, the probe is raised in small increments through the profile to above the soil surface. Ideally, the increments should be 1 cm, but never more than 5 cm. When the probe is at 50 cm or greater depths, neutrons do not escape to the atmosphere, and count rates should be fairly constant, fluctuating only within the statistically permissible limits of $\pm\sqrt{C}$. As the active centre of the probe approaches the soil surface, neutrons escape to the atmosphere and the count rate decreases slowly and later exponentially when the probe passes into the air (Refer to the data of Table IV, represented in Fig. 4).

TABLE IV. COUNT RATE AS A FUNCTION OF DEPTH FOR TWO HOMOGENEOUS MEDIA: WATER AND SOIL AT $\theta = 0.35$ cm^3 cm^{-3}

Depth (cm)	N (water) (cpm)	N (soil) (cpm)
100	157,230	67,100
90	157,110	67,030
80	157,130	66,880
70	157,020	66,950
60	156,890	67,230
50	157,150	67,310
40	156,970	68,910
30	157,080	68,370
20	157,160	67,250
15	157,020	68,630
12.5	157,240	66,870
10	157,000	64,150
7.5	156,540	59,800
5	145,230	54,360
2.5	125,810	42,550
0	75,440	29,120
–5 (in air)	30,770	26,670
–10 (in air)	15,300	14,590
–20 (in air)	5,110	5,670

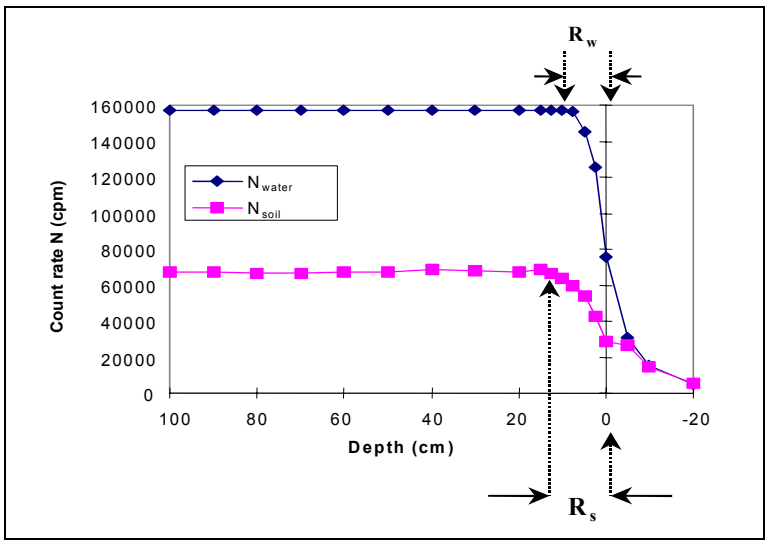

FIG. 4. Sphere-of-influence radius in soil and water.

Because of the escape of fast neutrons, the operator must take care to be self-protective, standing as far as possible from the probe.

From the graph of the count rate as a function of depth, the value of R_i is the depth at which the count rate starts to decrease. In this example, the radius of influence is approximately 10 cm in water and 15 cm in soil.

Falleiros (1994) recently extended the above methodology for heterogeneous soils and soils of variable water content. By using two sets of measurements–one with and one without the use of neutron deflector/absorbers–he was able to easily define the radius of influence.

2.6. Error analysis of determinations of soil-water content and storage

Clearly, as seen in Sections 2.1. and 2.2.2.1., the determination of soil-moisture by neutron moderation involves a series of physical processes. Starting with the production of fast neutrons and their moderation, through processes of detection, photomultiplication, discrimination, and counting, etc., the water content for a given soil depth is ascertained. Collectively, these processes determine the performance of a neutron probe. The set of errors collectively involved is the **instrument error**.

The count rate of neutrons slowed by interaction with water molecules in the soil can be considered physically proportional to the moisture content. These count rate, for practical purposes, have to be transformed into water-content values through a calibration curve based on a standard classical method for determining θ (Section 2.4.). In the calibration procedure, the primary errors that arise are those associated with the regression analysis relating cpm to θ. These errors depend on how representative are the water-content values measured within the sphere of influence of the probe. As previously discussed, the volume of the sphere depends upon the water content, source strength, soil variability (stratification and horizontal heterogeneity), installation of the access tubes, etc. This set of errors, included in the regression through calibration procedures, is called **calibration error**. These errors should be minimised by using procedures that ensure that the water-content determinations achieved through gravimetric methods are representative in relation to the count rates within the sphere of influence.

Once calibrated, the neutron probe can be used to measure soil-water content at any number of locations where access tubes are installed. Owing to the spatial variability of field soils, an exact measure of moisture content may require a different calibration curve for each location. If one calibration curve is used for several locations, the error involved are designated **local error**.

As will be seen later, each of these errors (instrument, calibration, local) can be separated into its components, some of which are readily identifiable and quantifiable with known models, whereas others are difficult to estimate. In Sections 2.6.1. and 2.6.2. we present the statistical methods for their study. Section 2.6.3. is devoted to the quantification of the error involved in the estimation of water storage in the soil profile. Two aspects affecting the estimation of soil-water are examined: the effect of the error in soil-water-content measurement and the influence of integration technique (trapezoidal and Simpson methods) on the estimation of soil-water storage.

2.6.1. Instrument and calibration errors

2.6.1.1. Linear regression

The information presented in Table V, calculated from the data provided in Table III, is needed to establish the linear regression between θ and CR. The resulting linear equation is the calibration curve. The calculation of the regression is made using the following equations:

$$a = \frac{\left(\sum CR^2\right)\left(\sum \theta\right) - \left(\sum CR\right)\left(\sum CR \times \theta\right)}{n\sum CR^2 - \left(\sum CR\right)^2} \tag{8}$$

$$a = \frac{\sum \theta}{n} = \frac{b\sum CR}{n} \tag{9}$$

$$b = \frac{n\sum CR \times \theta - \left(\sum CR\right)\left(\sum \theta\right)}{n\sum CR^2 - \left(\sum CR\right)^2} \tag{10}$$

$$R = \frac{\sum CR \times \theta - \left(\sum CR\right)\left(\sum \theta\right) \times n^{-1}}{\sqrt{\left[\sum CR^2 - \left(\sum CR\right)^2 \times n^{-1}\right] \times \left[\sum \theta^2 - \left(\sum \theta\right)^2 \times n^{-1}\right]}} \tag{11}$$

$$R = \frac{Cov(CR, \theta)}{\sqrt{\sigma^2(CR) \times \sigma^2(\theta)}} \tag{12}$$

where

n is the total number of measurement points
σ is the standard deviation

The slope, b, can be calculated directly from eq. (10). The intercept, a, can be obtained from eq. (9) or calculated directly from eq. (8). And eq. (11) enables the calculation of the **correlation coefficient** R, related to the concept of **covariance**: *Cov(CR,θ).*

To illustrate how these equations are used, we refer to the data in Table III. The intermediate calculations are indicated in Table V, in which $C\overline{R}$ and $\overline{\theta}$ are the average values for the count ratio and water content, respectively,

$$C\overline{R} = \frac{1}{n}\sum_{1}^{n} CR \text{ and } \overline{\theta} = \frac{1}{n}\sum_{1}^{n} \theta$$

Substituting the appropriate values from Table V into the above equations (with the help of Excel or Lotus), the regression equation of the calibration curve for this probe at this soil depth is

$$\theta = -0.09535 + 1.0423767CR$$

where

θ and CR are estimates of θ and CR, respectively.

Details of the statistical analysis are given in Table VI.

According to Greacen (1981), by taking the inverse regression $CR = a' + b'\theta$ and transforming it into the above calibration form $\theta = a + b \times CR$, the error in θ determination is decreased.

TABLE V. VALUES OF θ AND CR, AND CALCULATIONS NEEDED FOR THE ESTABLISHMENT OF THE CALIBRATION CURVE

No.	θ	CR [a]	$\theta \times CR$	$(CR)^2$	θ^2	$(CR-CR)^2$	$(\theta-\theta)^2$
1	0.424	0.507	0.21497	0.25705	0.17978	0.005806	0.004942
2	0.413	0.481	0.19865	0.23136	0.17057	0.002522	0.003516
3	0.393	0.485	0.19061	0.23523	0.15445	0.002938	0.001544
4	0.387	0.453	0.17531	0.20521	0.14977	0.000493	0.001108
5	0.378	0.432	0.16330	0.18662	0.14288	0.000001	0.000590
6	0.375	0.441	0.16538	0.19448	0.14063	0.000104	0.000453
7	0.306	0.377	0.11536	0.14213	0.09364	0.002894	0.002275
8	0.287	0.367	0.10533	0.13469	0.08237	0.004070	0.004448
9	0.291	0.395	0.11495	0.15603	0.08469	0.001282	0.003931
10	0.283	0.370	0.10471	0.13690	0.08009	0.003697	0.004998
Σ	3.537	4.308	1.5486	1.8797	1.2788	0.023806	0.027810
Average	0.354	0.431					

[a]Determined as in eq. (5). N_s in water = 157,050 cpm.

TABLE VI. RESULTS OF THE LINEAR REGRESSION
BASED UPON DATA PROVIDED IN TABLE V

Component	Datum
Intercept (a)	– 0.095356
Slope (b)	1.042377
Standard deviation of $\theta = \sigma(\theta)$	0.0156
Standard deviation of a = $\sigma(\alpha)$	0.0438
Standard deviation of $b = \sigma(b)$	0.101
Square of the correl'n coefft. (R^2)	0.930 (R = 0.96444)
Number of observations (n)	10
Degrees of freedom (n–2)	8

2.6.1.2. Analysis of variance

The analysis of variance of the regression is shown in Table VII. The values were calculated from the following equations:

$$SS_{total} = \sum \theta^2 - \frac{(\sum \theta)^2}{n} \tag{13}$$

$$SS_{regression} = \frac{\left[\sum(\theta \times CR) - \sum \theta \times \sum CR \times n^{-1}\right]^2}{\sum CR^2 - (\sum CR)^2 \times n^{-1}} \tag{14}$$

and $$SS_{residual} = SS_{total} - SS_{regression} \tag{15}$$

These are the sums of squares (denoted *SS*) and their differences from which means of squares (*MS*) are calculated.

TABLE VII. ANALYSIS OF VARIANCE OF THE REGRESSION

Causes of variation	Degrees of freedom	Sum of squares (*SS*)	Mean of squares (*MS*)	*F*
Regressio n	1	0.025866	0.025866	106.44
Residual	8	0.001944	0.000243	
Total	9	0.027810		

$\sqrt{MS_{residual}}$ indicates the standard deviation of the estimate of the water content from the calibration curve, i.e. $\sqrt{0.000243} \approx 0.0156$, per the third line in Table VI.

Whether the correlation coefficient R defined by eq. (11) or (12) differs significantly from zero is determined as follows:

– *t*-Test:

Using values of $R = 0.964$ and $n = 10$ in the following equation,

$$t = \frac{R\sqrt{n-2}}{1-\sqrt{1-R^2}} \tag{16}$$

we obtain a value of $t = 3.71$. From tables of probability for $(n - 2) = 8$, we have the following values of t for different levels of probability:

$t = 5.50$	0.1% (99.9% probability)
$t = 3.36$	1.0% (99.0% probability)
$t = 2.31$	5.0% (95.0% probability)

As 3.71 > 3.36, the correlation coefficient is significantly different from zero with a probability greater than 99%.

– *F*-Test:

Substituting the appropriate *MS* values from Table VII into the following equation,

$$F = \frac{MS_{regression}}{MS_{residual}} \tag{17}$$

we obtain

$$F = \frac{0.025886}{0.000243} \approx 106.44$$

which is much larger than 11.3, the value required for a significance of 1.0%.

Hence, both the *t*- and *F*-tests indicate that the correlation coefficient R defined by eq. (11) or (12) differs from zero with a probability greater than 99%.

2.6.1.3. Variance and covariance of the estimates of parameters a and b of the regression

Calculations of the variances, (σ^2), of the intercept and slope of the above regression, as well as their covariances *(Cov)*, using values provided in Tables V and VII, are given below.

$$\sigma^2(a) = \left\{\frac{1}{n} + \frac{(C\overline{R})^2}{\sum(CR - C\overline{R})^2}\right\} \times MS_{residual} \approx 0.00192$$

$$\sigma^2(b) = \frac{MS_{residual}}{\sum(CR - C\overline{R})^2} = \frac{0.000243}{0.0238} \approx 0.0102$$

The standard deviations of a and b, are $\sigma(a)$ (= $\sqrt{0.00192} \approx 0.0438$) and $\sigma(b)$ (= $\sqrt{0.0102} \approx 0.101$), respectively, as reported in Table VI. The covariance of a with b is

$$Cov(a,b) = \sigma(a,b) = \frac{C\overline{R} \times MS_{residual}}{\sum (CR - C\overline{R})^2} = \approx 0.00439$$

2.6.1.4. Total variance of θ (Haverkamp et al., 1984)

The regression equation obtained above contains estimated values of the real values of θ, CR, a and b, indicated by $\theta, CR, a,$ and b respectively. Hence, we have

$$\theta = a + b \times CR \qquad \text{(true)} \tag{18}$$

$$\theta = a + b \times CR + \varepsilon_0 \qquad \text{(estimated)} \tag{19}$$

where

the expected values are designated as $E(\theta) = \theta$, $E\{a\} = a$, $E\{b\} = b$, $E\{CR\} = CR$ and ε_0 is the estimation error of the regression.

The difference between the true value θ and its estimated value θ is

$$\theta - \theta = a - a + bCR - bCR + \varepsilon_0 \tag{20}$$

or, in another form

$$\theta - \theta = a - a + b(CR - CR) + CR(b - b) + \varepsilon_0 \tag{21}$$

The mathematical expectation of the square of this difference is

$$\begin{aligned} &E\{(\theta - \theta)^2\} = E\{(a-a)^2\} + E\{b^2(CR - CR)^2\} \\ &+ E\{CR^2(b-b)^2\} + E\{\varepsilon_0\} - 2E\{CR(a-a)(b-b)\} \end{aligned} \tag{22}$$

Equation (22) can be written as

$$\sigma^2(\theta) = \sigma^2(a) + [b^2 - \sigma^2(b)]\sigma^2(CR) + CR^2\sigma^2(b) + \sigma_0^2 - 2CR\sigma(a,b) \tag{23}$$

where

σ_0^2 is the variance of ε_0.

The variance $\sigma^2(CR)$ can be estimated from

$$\sigma^2(CR) = \left(\frac{N}{N_S}\right)^2 \left[\frac{\sigma^2(N)}{N^2} + \frac{\sigma^2(N_S)}{N_S^2}\right] \tag{24}$$

where

N and N_S are the counting rates in the soil and in the standard, obtained during selected counting times T and T_S, respectively.

Considering that the neutron-emission process follows Poisson's distribution, the variances associated with N and N_S are

$$\sigma^2(N) = \frac{N}{pT} \tag{25}$$

$$\sigma^2(N_S) = \frac{N_S}{qT_S} \tag{26}$$

where

p and q are the numbers of replicates of counts made in the soil and in the standard, respectively.

Substituting (25) and (26) into (24), we have

$$\sigma^2(CR) = \frac{1}{N_S}\left[\frac{CR}{pT} + \frac{CR^2}{qT_S}\right] \tag{27}$$

and substituting (27) into (23), the total variance of the estimated soil-water content becomes

$$\sigma^2(\theta) = \sigma^2(a) + \left[\frac{b^2 - \sigma^2(b)}{N_S}\right] \times \left[\frac{CR}{pT} + \frac{CR^2}{qT_S}\right] + CR^2\sigma^2(b) - 2CR\sigma(a,b) + \sigma_0^2 \tag{28}$$

This equation has two components, as follows.

– Variance due to calibration:

$$\sigma_C^2(\theta) = \sigma^2(a) + CR^2\sigma^2(b) - 2CR\sigma(a,b) + \sigma_0^2 \tag{29}$$

where

σ_0^2 is $SM_{residual}$ (see Table VII).

– Variance due to instrumental error:

$$\sigma_I^2(\theta) = \left[\frac{b^2 - \sigma^2(b)}{N_S}\right] \times \left[\frac{CR}{pT} + \frac{CR^2}{qT_S}\right] \tag{30}$$

Example: To calculate $\sigma_C^2(\theta)$ and $\sigma_I^2(\theta)$, we need the parameters a and b and their variances and co-variances. We also need a set of neutron-probe measurements at one location, in the same access tube, and at one chosen depth. To convert them into CR and to calculate CR (estimated mean value), we need standard measurements also. Table VIII provides the necessary information.

TABLE VIII. REPLICATED DATA FROM A NEUTRON PROBE PLACED AT 60 cm IN A SINGLE ACCESS TUBE AND ONE STANDARD MEASUREMENT IN WATER

Replicates	*C* (counts)	*T* (min)	*N* (cpm)	*CR*
1	140,800	2	70,400	0.444
2	138,200	2	69,100	0.436
3	140,500	2	70,250	0.443
4	139,900	2	69,950	0.441
5	139,100	2	69,550	0.439
Mean	139,700	2	69,850	0.440
Standard (water)	317,000	2	158,500	

Using equations (25) and (26),

$$\sigma^2(N) = \frac{69{,}850}{5\times 2} = 6{,}985$$

$$\sigma^2(N_S) = \frac{158{,}500}{1\times 2} = 79{,}250$$

and from eq. (24),

$$\sigma^2(CR) = \left(\frac{69{,}850}{158{,}500}\right)^2 \left(\frac{6{,}985}{69{,}850^2} + \frac{79{,}250}{158{,}500^2}\right) \approx 8.9\times 10^{-7}$$

It is important to note that eq. (27) shows that, by increasing the number of replicates *p* and *q* as well as counting times *T* and T_S, the variances will decrease. Counting for a longer time has the same effect as increasing the number of replicates. It is noteworthy also that some modern neutron probes show only count rates *N*, and do not show accumulated counts *C*. Nevertheless, the above considerations remain valid and indicate that variance of the count rate decreases whenever the number of replicates and/or the counting time increases.

We now calculate the calibration and the instrumental variances of the measured soil-water content. Using the mean value of *CR* = 0.440 (Table VIII) in the calibration equation (Table VI), we have

$$\theta = -0.0953 + 1.04\times 0.440 \approx 0.364$$

Equation (29) enables the calculation of the variance due to calibration error. Utilizing $\sigma^2(\hat{a}) = 0{,}00192$, $\sigma^2(\hat{b}) = 0{,}0102$, $Cov(a,b) = 0{,}004398$ (Section 2.6.1.1.) and $MS_{residual}$ = 0.000243 (Table VII), the calibration variance of the soil-water content is

$$\sigma_C^2(\theta) = 0.00192 + 0.0102\times 0.440^2 - 2\times 0.440\times 0.00439 + 0.000243 = 2.68\times 10^{-4}$$

The standard deviation due to calibration is

$$\sigma_C(\theta) = \sqrt{2.68\times10^{-4}} = 1.64\times10^{-2}$$

The coefficient of variation owing to calibration is

$$CV\% = \frac{100\times\sigma_C(\theta)}{\theta} = \frac{100\times1.64\times10^{-2}}{0.364} \approx 4.5\%$$

Instrument variance of the soil-water content from eq. (30) is

$$\sigma_I^2(\theta) = \left(\frac{1.042^2 - 0.102}{158{,}500}\right)\times\left(\frac{0.440}{5\times2} + \frac{0.440^2}{1\times2}\right) \approx 9.58\times10^{-7}$$

The standard deviation due to the instrument is

$$\sigma_I(\theta) = \sqrt{9.58\times10^{-7}} \approx 9.79\times10^{-4}$$

The coefficient of variation owing to the instrument is

$$CV\% = \frac{100\times9.79\times10^{-4}}{0.364} \approx 0.27\%$$

Total variance of soil-water content for θ = 0.364 is

$$\sigma^2(\theta) = \sigma_C^2(\theta) + \sigma_I^2(\theta) = 2.68\times10^{-4} + 9.58\times10^{-7} \approx 2.69\times10^{-4}$$

The total standard deviation is

$$\sigma(\theta) = \sqrt{2.69\times10^{-4}} \approx 1.64\times10^{-2}$$

The coefficient of total variation is

$$CV\% = \frac{100\times1.64\times10^{-2}}{0.364} \approx 4.5\%$$

These results show that calibration errors are much more important than instrument errors. Any attempt to decrease the total variance should focus on the calibration procedure. It is noteworthy that the above analysis is valid for only one access tube at one selected soil depth. We now consider the variance of several measurements taken at one depth in several different access tubes.

2.6.2. Local error

Measuring soil-water content with replicates of *CR* obtained in different access tubes installed randomly in a field, we obtain a mean value, $<\theta>$, that has another variance component corresponding to the spatial variability of the soil within the field. The local

variance due to the location of the measurement within the field (Vauclin et al., 1984) is given by

$$\sigma_L^2(<\theta>) = \frac{\sigma^2(L)}{k}\left[\frac{b^2 - \sigma^2(b)}{N_S}\right] \tag{31}$$

where

$\sigma^2(L)$ is the variance owing to soil spatial variability,
and k is the number of point measurements of θ.

Owing to difficulties involved in the determination of $\sigma^2(L)$, the same authors suggested that $\sigma_L^2(<\theta>)$ be calculated by difference, according to

$$\sigma_L^2(<\theta>) = \sigma^2(<\theta>) - \sigma_C^2(<\theta>) - \sigma_I^2(<\theta>) \tag{32}$$

By analogy to eq. (23), the above equation becomes

$$\begin{aligned}\sigma^2(<\theta>) = {} & [b^2 - \sigma^2(b)]\sigma^2(<C\overline{R}>) + \sigma^2(a) \\ & + (<C\overline{R}>)^2\sigma^2(b) - 2<C\overline{R}>\sigma(a,b)\end{aligned} \tag{33}$$

where

$\sigma_0^2 = MS_{residual} = 0$ because it is the variance of a mean value.

The value of $\sigma^2(<C\overline{R}>)$,

$$\sigma^2(<C\overline{R}>) = \frac{\sigma^2(CR)}{k} \tag{34}$$

accounts for local variability and represents the mean of the variance of k measurements of CR in k access tubes taken at the same depth.

Example: CR values, measured in a set of thirty access tubes at 20 cm depth in a "homogeneous" field, are shown in Table IX. They were determined as in eq. (5) with T = 1 min, T_S = 1 min and N_S in water=157,050 cpm, with one count of p (in soil) and of q (in standard). Five measurements (k = 5), selected at random, corresponding to access tubes 6, 14, 26, 29 and 30, are shown in Table X.

$$\sigma^2(CR) = \frac{\sum(CR - C\overline{R})^2}{k} = \frac{3.74\times10^{-3}}{5} \approx 7.48\times10^{-4}$$

$$\sigma^2(<C\overline{R}>) = \frac{7.48\times10^{-4}}{5} \approx 1.50\times10^{-4}$$

Using the values of $a, \sigma^2(a)$, $b, \sigma^2(b)$, *and* $Cov(a,b)$ determined in Section 2.6.1.1., the total variance of soil-water content is calculated as

$$\sigma^2(<\theta>) = 2.16\times10^{-4}$$ [cf. eq. (33)]

The instrument variance is

$$\sigma_I^2(<\theta>) = 2.28\times10^{-6}$$ [cf. eq. (30)]

And calibration variance is

$$\sigma_C^2(<\theta>) = 5.47\times10^{-5}$$ [cf. eq. (29) without σ_0^2]

Local or spatial variability variance is obtained by difference as follows:

$$\sigma_L^2(<\theta>) = 2.16\times10^{-4} - 2.28\times10^{6} - 5.47\times10^{-5} \approx 1.6\times10^{-4}$$ [cf. eq. (32)]

If the calculations above are repeated for different sets of measurements of varying *k*, it will be observed that instrument variance is always very small compared to the others, and that the calibration variance is fairly constant because it is not affected by *k*. On the other hand, the local variance, and hence the total variance, will decrease with increasing *k*. Because this decrease levels off as *k* increases (Table XI and Fig. 5), it is possible to define the ideal number of access tubes (*k*) to yield a desired coefficient of variation in the water content.

TABLE IX. CR DATA OBTAINED AT 20-cm DEPTH IN THIRTY NEUTRON-PROBE ACCESS TUBES INSTALLED IN AN ALFISOL AT PIRACICABA, BRAZIL

Tube	$C\hat{R}$	Tube	$C\hat{R}$
1	0.476	16	0.460
2	0.507	17	0.511
3	0.508	18	0.490
4	0.515	19	0.488
5	0.515	20	0.486
6	0.535	21	0.489
7	0.528	22	0.497
8	0.513	23	0.479
9	0.494	24	0.467
10	0.504	25	0.485
11	0.469	26	0.452
12	0.497	27	0.487
13	0.484	28	0.485
14	0.487	29	0.478
15	0.477	30	0.475
			$<\hat{\overline{CR}}>= 0.491$

T=1', T_s=1', p=1, q=1, N_s in water = 157,050 cpm.

For the thirty measurements of Table IX, $< C\overline{R} >= 0.4914$ corresponds to an estimated soil-water content value of $< \theta >= 0.417$ from the calibration equation. Considering 30 to be a very large value for k, we take 0.417 as the true value of θ. How many access tubes would be needed to measure the water content with a CV of 3%?

$$CV\% = \frac{100\sigma(< \overline{\theta} >)}{< \overline{\theta} >} \quad \text{or} \quad \sigma(< \overline{\theta} >) = \frac{< \overline{\theta} > (CV\%)}{100}$$

$$\sigma(< \overline{\theta} >) = \frac{3 \times 0.417}{100} \leq 1.25 \times 10^{-2} \quad \text{or} \quad \sigma^2(< \overline{\theta} >) = \leq 1.56 \times 10^{-4}$$

The first and fourth columns of Table XI show that k should be between 5 and 10. Refining the data of Table XI for more values of k, we conclude that the use of six access tubes provides a CV equal to 3%.

TABLE X. CR DATA FOR FIVE (k=5) RANDOM ACCESS TUBES FROM TABLE IX

Tube	CR	$(CR - C\overline{R})^2$
6	0.535	2.46×10^{-3}
14	0.487	2.56×10^{-6}
26	0.452	1.12×10^{-3}
29	0.478	5.48×10^{-5}
30	0.475	1.08×10^{-4}
		$\sum = 3.74 \times 10^{-3}$

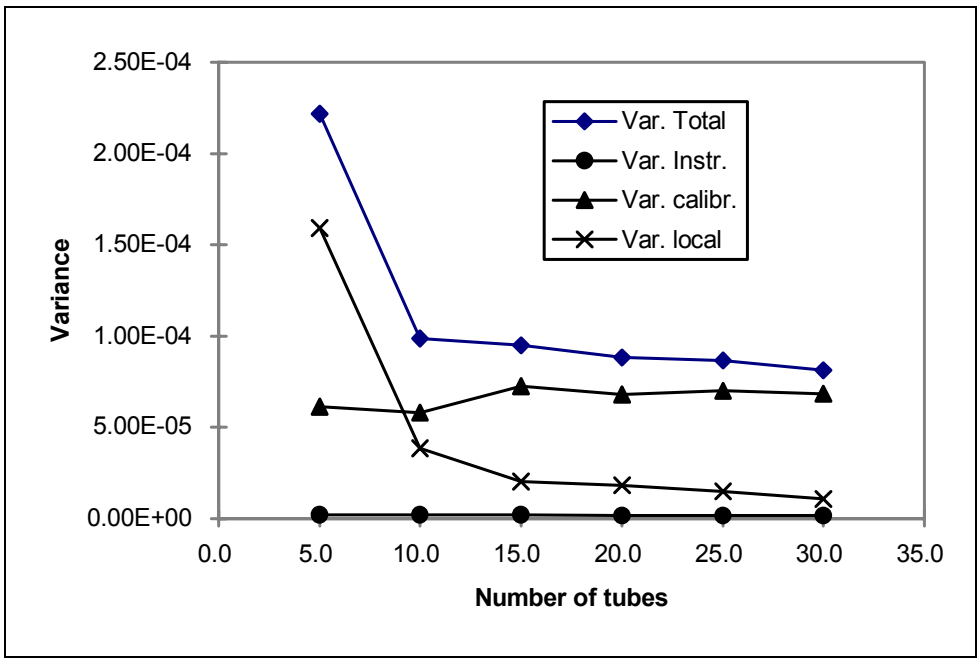

FIG. 5. Total and component variances of $\overline{\theta}$ as a function of number of access tubes (k) calculated using data from Table IX.

TABLE XI. VARIANCE COMPONENTS OF $\overline{\theta}$ AS A FUNCTION OF THE NUMBER OF ACCESS TUBES (k)

k	Access tube	$\sigma^2(<C\overline{R}>)$ ($\times 10^{-4}$)	$\sigma^2(<\overline{\theta}>)$ ($\times 10^{-4}$)	$\sigma_I^2(<\overline{\theta}>)$ ($\times 10^{-6}$)	$\sigma_C^2(<\overline{\theta}>)$ ($\times 10^{-5}$)	$\sigma_L^2(<\overline{\theta}>)$ ($\times 10^{-4}$)
5	6, 14, 26, 29, 30	1.496	2.158	2.32	5.47	1.601
6	5, 7, 22, 26, 28, 30	1.052	1.758	2.38	6.25	1.124
7	3, 5, 8, 9, 12, 13, 25	0.200	0.939	2.44	7.24	0.208
10	4, 5, 9, 11, 15, 20, 23, 24, 26, 30	0.371	0.919	2.30	5.20	0.394
15	2, 3, 5, 7, 8, 9, 10, 12,16, 18, 19, 24, 27, 28, 30	0.204	0.881	2.40	6.60	0.216
20	1, 2, 3, 4, 5, 6, 9, 11, 13, 14, 15, 16, 17, 18, 19, 20, 22, 23, 26, 28	0.188	0.815	2.37	6.12	0.200
25	All except 1, 3, 13, 15, 28	0.156	0.800	2.38	6.32	0.166
30	All	0.118	0.745	2.37	6.18	0.125

2.6.3. Errors in the calculation of soil-water storage

To calculate the amount of water stored in a soil profile, we integrate the measured moisture contents from the surface to the desired depth, z, hence, there are errors owing to θ measurements and the integration method. **Soil-water storage** at a given time is

$$S = \int_0^z \theta(z)dz \tag{35}$$

Because the function $\theta(z)$ is not known analytically, S is calculated numerically. Here we shall make the integration with two commonly used numerical approaches, the "trapezoidal" method and "Simpson's" method.

Considering that the total variance on the estimated water storage $\sigma^2(S)$ has one component, $\sigma_1^2(S)$, related to the error in water content and another, $\sigma_2^2(S)$, which is inherent in the integration utilized, thus:

$$\sigma^2(S) = \sigma_1^2(S) + \sigma_2^2(S) \tag{36}$$

where

$\sigma_1^2(S)$ is the soil-water-content variance,
and $\sigma_2^2(S)$ is the integration variance.

2.6.3.1. Trapezoidal method

Figure 6 shows a profile for which the water storage S is calculated using the **trapezoidal method**.

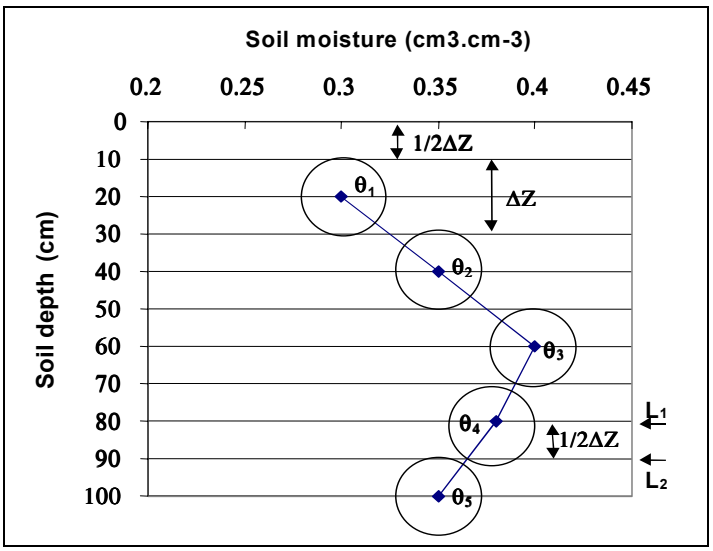

FIG. 6. Soil-water-content profile from neutron-probe measurements at 20-cm intervals.

With this method, profile shown in Fig. 6 is obtained by linear interpolation between the points. To evaluate the soil water content in each layer of soil (z_i, z_{i+1}) of thickness Δz, the surface of a trapezoid is calculated [in this case $(\theta_i + \theta_{i+1}) \times \Delta z/2$] from which the name of the method is derived. If the individual contributions of a profile consisting of n layers of the same thickness Δz are summed, the following general formula is obtained:

$$S = \sum_{i=0}^{n-1} (\theta_i + \theta_{i+1}) \times \frac{\Delta z}{2} = \left[\frac{1}{2}\theta_0 + \theta_1 + \ldots + \theta_i + \ldots + \theta_{n-1} + \frac{1}{2}\theta_n \right] \times \Delta z \tag{37}$$

In the example shown in Fig. 6, if the integration of S is made at $L_1 = -80$ cm (centre of the sphere of influence), and assuming that the water content at the surface θ_0 is equivalent to θ_1 measured at –20 cm, we have

$$S_{L_1} = (1.5\theta_1 + \theta_2 + \theta_3 + 0.5\theta_4)\Delta z \tag{38}$$

and if the integration is extended until $L_2 = -90$ cm, considering that θ_4 remains at that level (same sphere of influence), we will have

$$S_{L_2} = (1.5\theta_1 + \theta_2 + \theta_3 + \theta_4)\Delta z \tag{39}$$

remembering that

$$\sigma^2(a+b) = \sigma^2(a) + \sigma^2(b) \tag{40}$$

and $$\sigma^2(kx) = k^2\sigma^2(x) \tag{41}$$

in which k is a constant, we have the variances of the soil-water storage including only the errors due to the measurement of θ for depths of integration to L_1 and L_2, respectively,

$$\sigma_1^2\left(S_{L_1}\right) = [1.5^2\sigma^2(\theta_1) + \sigma^2(\theta_2) + \sigma^2(\theta_3) + 0.5^2\sigma^2(\theta_4)](\Delta z)^2 \tag{42}$$

$$\sigma_2^2\left(S_{L_2}\right)=[1.5^2\sigma^2(\theta_1)+\sigma^2(\theta_2)+\sigma^2(\theta_3)+\sigma^2(\theta_4)](\Delta z)^2 \quad (43)$$

The integration variance is due to the interpolation error, which is overestimated according to Carnahan et al. (1969) with the trapezoidal integration method:

$$\sigma_2^2\left(S\right)=\frac{L^2(\Delta z)^4}{144}[\theta''(z)]^2 \quad (44)$$

where

$\theta''(z)$ is the second derivative of $\theta(z)$.

The value of the second-order derivative must be calculated, where possible, for each depth (at least one measurement point above and one below the depth under consideration), and the final value is be the variance estimated with the highest value obtained for $\theta''(z)$.

2.6.3.2. Simpson's integration method

With **Simpson's method**, the profile is interpolated by pieces of modified parabolas, layer by layer, on three points. The soil-water storage *S* to depth *L* (Carnahan et al., 1969) is as follows:

$$S=\int_0^L\theta(z)dz=\left[\frac{1}{3}\theta_0+\frac{4}{3}\theta_1+\frac{2}{3}\theta_2+\frac{4}{3}\theta_3+\ldots+\frac{2}{3}\theta_i+\frac{4}{3}\theta_{i+1}+\ldots+\frac{2}{3}\theta_{2n-2}+\frac{4}{3}\theta_{2n-1}+\frac{1}{3}\theta_{2n}\right]\times\Delta z \quad (45)$$

where

$2n$ is the number of soil layers of thickness Δz ($n \geq 2$)
and n is the number of fourth-order derivatives.

Because the number of soil layers ($2n$) within the limits of integration (0 to L) has to be even, the number of observations (2n + 1)of θ has to be odd, and not less than five.

If we reconsider the example in the previous paragraph over the horizon (0, –80 cm) with the same hypothesis $\theta_0 = \theta_1$, eq. (45) becomes

$$S_{l_1}=\left[\frac{5}{3}\theta_1+\frac{2}{3}\theta_2+\frac{4}{3}\theta_3+\frac{1}{3}\theta_4\right]\times\Delta z \quad (46)$$

Per eq. (45), the soil-water storage variance due to error of measurement of water content is

$$\sigma_1^2\left(S\right)=\left(\frac{\Delta z}{3}\right)^2\left[\sigma^2(\theta_0)+4^2\sigma^2(\theta_1)+2^2\sigma^2(\theta_2)+4^2\sigma^2(\theta_3)+\ldots\right.$$
$$\left.+2^2\sigma^2(\theta_4)+\quad+2^2\sigma^2(\theta_{2n-2})+4^2\sigma^2(\theta_{2n-1})+\sigma^2(\theta_{2n})\right] \quad (47)$$

The constants that multiply $\theta(z)$ and $\sigma^2(\theta)$ in the expressions of S and $\sigma_1^2(S)$ are defined by Simpson's rule.

The soil-water-storage error due to the integration by Simpson's method is

$$\sigma_2(S) = \frac{(\Delta z)^5}{90} \sum_{i=1}^{n} \theta''''(z_i) \tag{48}$$

Squaring both sides of the above equation and remembering that $L = 2n\Delta z$, we have

$$\sigma_2^2(S) = \left[\frac{2n\Delta z(\Delta z)^4 \theta''''(z)}{2 \times 90} \right]^2 = \frac{L^2(\Delta z)^8}{180^2} [\theta''''(z)]^2 = \frac{L^2(\Delta z)^8}{32{,}400} [\theta''''(z)]^2 \tag{49}$$

Hence, the variance is

$$\sigma_2^2(S) = \frac{L^2(\Delta z)^8}{32{,}400} [\theta''''(z)]^2 \qquad \text{and}$$

$$\theta''''(z) = \frac{\Delta^4 \theta}{4!(\Delta z)^4} \tag{50}$$

where

$\Delta^4\theta$ is the fourth-order difference in θ.

The indices of $\theta(z)$ in the fourth-order derivatives are determined using Pascal's Triangle (Table XII).

TABLE XII. PASCAL'S TRIANGLE

Number of points	$\Delta\theta$ of Order n $\Delta^n\theta$	Order of $\Delta\theta$
1	$+1\,\theta_1$	---
2	$+1\,\theta_1 \quad -1\,\theta_0$	1
3	$+1\,\theta_2 \quad -2\,\theta_1 \quad +1\,\theta_0$	2
4	$+1\,\theta_3 \quad -3\,\theta_2 \quad +3\,\theta_1 \quad -1\,\theta_0$	3
5	$+1\,\theta_4 \quad -4\,\theta_3 \quad +6\,\theta_2 \quad -4\,\theta_1 \quad +1\,\theta_0$	4
	And successively	

2.6.3 3. Soil-water-storage variance calculations

Table XIII presents soil-water-content data measured at twenty-five locations using access tubes with the same probe, in 25-cm depth increments from the soil surface to 150 cm. With these data, we will make the calculations, using the integration methods, already presented.

2.6.3.3.1. Trapezoidal method

Soil water storage to a depth of 150 cm is

$$S_{150} = 25(1.5\times 0.336 + 0.347 + 0.325 + 0.296 + 0.5\times 0.297) \qquad \text{[cf. eq. (37)]}$$

S_{150} = 47.99 cm or 479.9 mm.

Soil-water-storage variance due to θ measurements is

$$\sigma_1^2(S_{150}) = (1.5^2\times 0.00086 + 0.00106 + 0.00031 + 0.00019 + 0.00030 + 0.5^2\times 0.00028)\times 25^2 \approx 2.41 \qquad \text{[cf. eq. (42)]}$$

$$\sigma_1^2(S_{150}) = 2.41$$

Therefore, the standard deviation is

$$\sigma_1(S_{150}) = \sqrt{2.41} \approx 1.55 \text{ cm or } 15.5 \text{ mm}$$

The soil-water-storage variance due to the integration method is

$$\sigma_2^2(S_{150}) = \frac{150^2\times 25^4}{144}[\theta''(z)]^2 \qquad \text{[cf. eq. (44)]}$$

The indices of $\theta(z)$ in the second-order derivatives are determined using Pascal's Triangle in Table XII as follows:

$$50\text{cm: } \theta''_{50} = \frac{0.325 - 2\times 0.347 + 0.336}{25^2} = -5.3\times 10^{-5}$$

$$75\text{ cm: } \theta''_{75} = \frac{0.300 - 2\times 0.325 + 0.347}{25^2} = -4.7\times 10^{-6}$$

$$100\text{ cm: } \theta''_{100} = \frac{0.296 - 2\times 0.300 + 0.325}{25^2} = 3.3\times 10^{-5}$$

$$150\text{ cm: } \theta''_{150} = \frac{0.297 - 2\times 0.296 + 0.300}{25^2} = 8.0\times 10^{-6}$$

The largest value of $|\theta''(z)|$ is 5.3×10^{-5} occurring at z = 50 cm. Therefore,

$$\sigma_2^2(S_{150}) = \frac{150^2 \times 25^4}{144}\left[-5.3\times10^{-5}\right]^2 = 1.7\times10^{-1}$$

and the standard deviation is

$$\sigma_2(S_{150}) = \sqrt{1.7\times10^{-1}} = 0.4123\,\text{cm} = 4.12\ \text{mm}$$

The total variance of soil-water storage is calculated as follows,

$$\sigma^2(S_{150}) = \sigma_1^2(S_{150}) + \sigma_2^2(S_{150}) = 2.41 + 0.17 = 2.58$$

and, therefore, the standard deviation is

$$\sigma(S_{150}) = \sqrt{2.58} = 1.61\ \text{cm} = 16.1\ \text{mm}$$

2.6.3.3.2. Simpson's method

In order to use Simpson's integration method, an even number of soil layers ($2n$) must be analyzed from the soil surface to the maximum integration depth, and, therefore, there is an odd number of measurements of θ. Inasmuch as six average values of θ were presented in Table XIII, it is necessary to consider an additional value: the value of θ at the soil surface is assumed to be equal to the measurement made at 25 cm.

Hence, the estimated amount of water stored in the 150-cm profile is

$$S_{150} = \frac{25}{3}\times[\ 0.336 + 4\times0.336 + 2\times0.347 + 4\times0.325 + 2\times0.300 + 4\times0.297\ ]$$

[cf. eq. (45)]

$$S_{150} = 47.93\,\text{cm} = 479.3\,\text{mm}$$

The variance due to θ measurements is

$$\sigma_1^2(S_{150}) = \left(\frac{25}{3}\right)^2 (0.00086 + 4^2\times0.00086 + 2^2\times0.00106 + 4^2\times0.00031 + 2^2\times0.00019 + 4^2\times0.00030 + 0.00028) \approx 2.06$$

[cf. eq. (47)]

and the standard deviation is

$$\sigma_1(S_{150}) = \sqrt{2.06} = 1.435\ \text{cm} = 14.35\,\text{mm}$$

The soil-water-storage variance due to the integration method is

$$\sigma_2^2(S_{150}) = \frac{150^2 \times 25^8}{32{,}400}[\theta''''(z)]^2$$

[cf. eq. (49)]

The indices of $\theta(z)$ in the fourth-order derivatives are determined using Pascal's Triangle (Table XII). In this example, as we have seven measurement points and we need five for the calculation of the fourth-order derivatives, it is possible to calculate only three values – for depths of 50, 75 and 100 cm. We use the coefficients provided in Pascal's Triangle, in this case those in the last line of Table XII.

$$\theta''''(50) = \frac{(\theta_4 - 4\theta_3 + 6\theta_2 - 4\theta_1 + \theta_0)}{4!(\Delta z)^4}$$

$$\theta''''(75) = \frac{(\theta_5 - 4\theta_4 + 6\theta_3 - 4\theta_2 + \theta_1)}{4!(\Delta z)^4}$$

$$\theta''''(100) = \frac{(\theta_6 - 4\theta_5 + 6\theta_4 - 4\theta_3 + \theta_2)}{4!(\Delta z)^4}$$

TABLE XIII. SOIL-WATER-CONTENT DATA MEASURED IN 25-cm STEPS WITH A NEUTRON PROBE FOR TWENTY-FIVE ACCESS TUBES TO A DEPTH OF 150 cm

Tube	25 cm	50 cm	75 cm	100 cm	125 cm	150 cm
1	0.372	0.393	0.383	0.344	0.304	0.293
2	0.378	0.393	0.347	0.308	0.300	0.313
3	0.359	0.352	0.327	0.317	0.300	0.300
4	0.379	0.374	0.309	0.288	0.293	0.299
5	0.362	0.353	0.320	0.288	0.284	0.285
6	0.358	0.336	0.316	0.301	0.281	0.296
7	0.315	0.337	0.316	0.291	0.291	0.293
8	0.365	0.393	0.345	0.298	0.287	0.292
9	0.315	0.334	0.312	0.300	0.305	0.338
10	0.362	0.382	0.355	0.316	0.315	0.332
11	0.357	0.358	0.316	0.291	0.364	0.281
12	0.361	0.370	0.327	0.294	0.276	0.282
13	0.346	0.343	0.317	0.297	0.300	0.290
14	0.348	0.347	0.307	0.278	0.283	0.274
15	0.332	0.335	0.335	0.298	0.288	0.289
16	0.323	0.338	0.323	0.295	0.290	0.315
17	0.291	0.311	0.312	0.310	0.296	0.306
18	0.326	0.345	0.336	0.324	0.303	0.295
19	0.328	0.384	0.336	0.296	0.286	0.286
20	0.285	0.234	0.306	0.291	0.289	0.278
21	0.340	0.334	0.308	0.287	0.286	0.292
22	0.294	0.339	0.310	0.285	0.286	0.287
23	0.315	0.326	0.314	0.295	0.282	0.288
24	0.301	0.325	0.323	0.308	0.317	0.335
25	0.283	0.333	0.319	0.298	0.287	0.297
Average	0.336	0.347	0.325	0.300	0.296	0.297
σ^2	0.00086	0.00106	0.00031	0.00019	0.00030	0.00028

We calculate and select the greatest value of $\theta''''(z)$, which occurs at $z = 50$,

$$\theta''''(50) = \frac{0.300 - 4\times 0.325 + 6\times 0.347 - 4\times 0.336 + 0.336}{4!25^4} \approx 7.89\times 10^{-9}$$

Therefore, we have the variance owing to the integration method,

$$\sigma_2^2\left(S_{150}\right) = \frac{150^2 \times 25^8}{32{,}400}(7.89\times 10^{-9})^2 \approx 6.59\times 10^{-6}$$

and the standard deviation is

$$\sigma_2\left(S_{150}\right) = \sqrt{6.59\times 10^{-6}} = 2.57\times 10^{-3}\,\text{cm} = 0.026\ \text{mm}$$

The total variance of soil-water storage is

$$\sigma^2\left(S_{150}\right) = \sigma_1^2\left(S_{150}\right) + \sigma_2^2\left(S_{150}\right) = 2.06 + 6.59\times 10^{-6} \approx 2.06$$

and the standard deviation is

$$\sigma\left(S_{150}\right) = \sqrt{2.06} = 1.43\ \text{cm} = 14.3\ \text{mm}$$

A summary of the soil-water-storage calculations is given in the following table.

Method	S_{150}	$\sigma_1^2(S_{150})$	$\sigma_2^2(S_{150})$	$\sigma^2(S_{150})$	$\sigma(S_{150})$
Trapezoidal	47.99	2.41	0.170	2.58	1.61
Simpson	47.93	2.06	6.59×10^{-6}	2.06	1.43

In this example, it is noteworthy that the variance due to θ measurements is far larger than that of the integration method. Both integration methods yield very similar results for soil-water storage with a smaller variance with Simpson's method.

3. NEUTRON/GAMMA PROBES FOR SIMULTANEOUS MEASUREMENT OF SOIL BULK DENSITY AND WATER CONTENT

3.1. General characteristics

In addition to the depth neutron probes described in Chapter 2, others allow the simultaneous measurement of soil bulk density and water content. For this purpose, they have a fast neutron source (often $^{241}Am + {}^{9}Be$) with a slow neutron detector (^{3}He chamber), and a gamma ray source (often ^{137}Cs) with a Geiger-Mueller-type detector. Depth probes and surface probes are available. Depth probes require the installation of access tubes in the soil profile. Surface probes measure the average water content of the surface layer (0–15 cm) and the bulk density of various layers of 2.5- to 30-cm thickness depending on the probe model. Soil-water-content measurements and calibration procedures for surface probes are identical to those described in Chapter 2 except that the fast-neutron source and slow-neutron detector are fixed to the base of the shield, precluding measurements at various soil depths. With respect to bulk-density measurements, depth probes rely on backscattering of gamma radiation, whereas surface probes rely both on backscattering and on attenuation of gamma radiation.

This chapter focuses on surface probes used to measure soil bulk density by backscattering as well as by attenuation. With slight modification, the discussion applies also to depth neutron/gamma probes.

Figures 7a and 7b show a surface neutron/gamma probe with its gamma source in two modes of operation. In mode (a), the gamma source is not lowered into the soil and can occupy two positions: BS (backscattering), a little above soil surface, and AC (asphalt-concrete) at the soil surface. Measurements in both positions are made by backscattering only, and the bulk-density evaluation is made on the surface layer. In mode (b), the gamma source is lowered into the soil to the desired depth (from 5 to 30 cm in 2.5-cm steps) and the bulk density is measured by both processes, gamma ray backscattering and gamma ray attenuation. For both modes of operation, (a) and (b), the average soil-water content of the soil surface (0–15 cm) is measured by neutron moderation, using a neutron source placed on the soil surface.

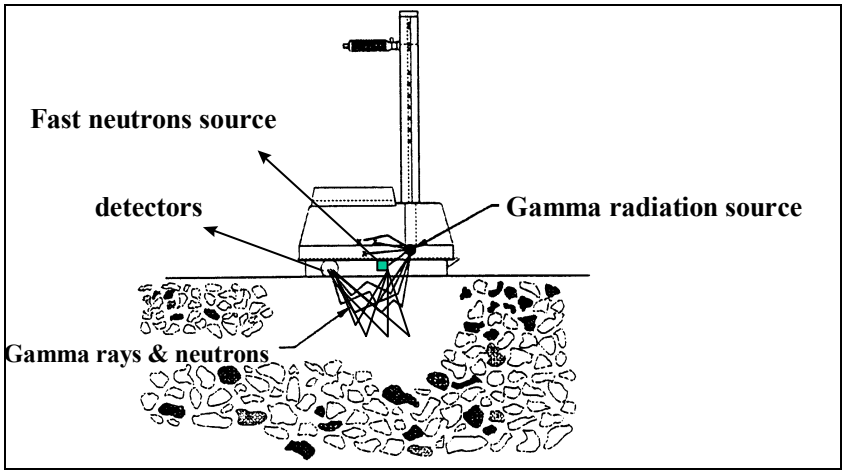

FIG. 7a. Probe in position to measure soil-water content and bulk density of the surface layer, by backscattering only.

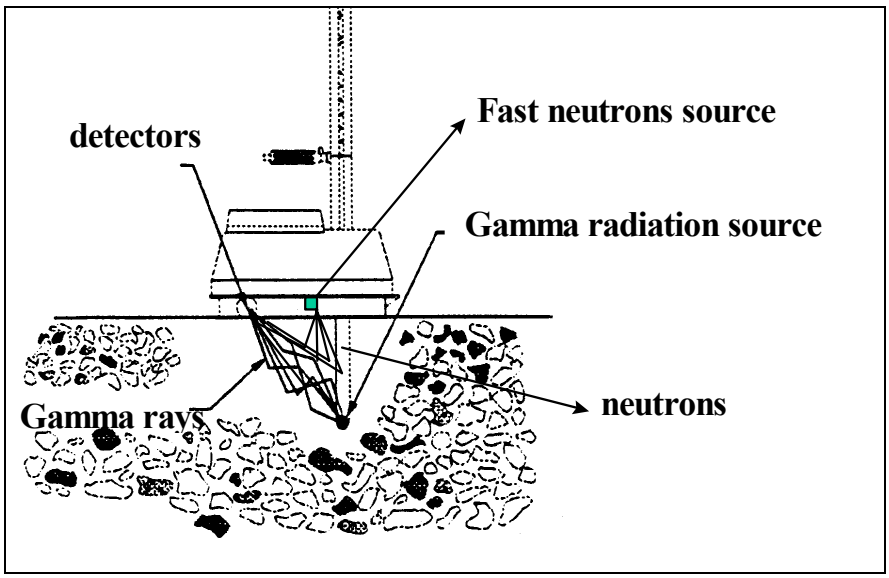

FIG. 7b. Probe in position to measure water content of the surface layer and bulk density to a desired depth, by attenuation and backscattering.

In these probes, the fast-neutron source is fixed to the base of the shield in such a way that, when in contact with the soil, the source is located at the probe/soil interface. The gamma ray source is located at the tip of a movable stainless-steel rod that permits its introduction into the soil down to the desired depth through a hole previously made with a small auger furnished by the manufacturer. Both gamma ray and slow-neutron detectors (Geiger-Mueller and ^{3}He) remain together at a fixed position at the base of the shield near the probe/soil interface when the probe is on the soil. The working principle for surface neutron/gamma probes is the same as for depth probes as discussed in Chapter 2, with only a hemisphere of influence of radius approximately 15 cm.

3.2. Working principle

As already mentioned, for the measurement of soil bulk density, surface probes use two physical processes: a) gamma-radiation backscattering and b) gamma ray attenuation.

3.2.1. Backscattering

For surface measurements of bulk density of soil and other materials such as concrete or asphalt paving, as shown in Fig. 7a, the gamma ray detector measures the photons that return to the soil surface after interacting (backscattering) with atoms of soil particles. The number of back-scattered photons is related to the density of the medium, as in Fig. 8.

In the useful range for measurement of bulk density (Fig. 8), the relation between medium bulk density, d'_b, and the back-scattered photon-count ratio, C, follows the model according to

$$d'_b = B \ln\left(\frac{A}{CR - C}\right) \tag{51}$$

where A, B and C are parameters determined experimentally using materials of known density, as indicated in Table XIV and Fig. 9, and CR is the count ratio (back-scattered photon count in the soil/standard density count).

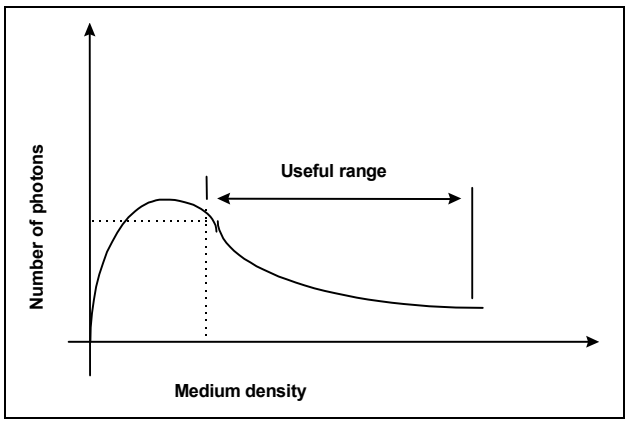

FIG. 8. Effect of medium density on the number of "reflected" photons.

If the soil is moist, part of the measured back-scattered radiation is caused by the water. The dry-soil bulk density, d_b, is related to the wet-soil bulk density, d'_b, by the relation

$$d_b = d_b^{'} - \rho_w \theta \tag{52}$$

where

ρ_w is the specific weight of water (g cm^{-3}).

For practical purposes, taking ρ_w = 1g cm^{-3}, we have

$$d_b = d_b^{'} - \theta \tag{53}$$

Inasmuch as the probe simultaneously measures θ through neutron moderation, the value of the dry bulk density is readily available.

3.2.2. Attenuation

When measurements are made at depth, as in Fig. 7b, the gamma ray detector counts both the number of photons that cross the soil sample of thickness X located between the gamma ray source and the detector, and the number of back-scattered gamma rays. Therefore, only some of the photons that reach the detector, after crossing the soil, can be associated to the Beer-Lambert's law of attenuation, according to eq. (54).

$$I = I_0 \exp[-(\mu_w \theta + \mu_s d_b) X] \tag{54}$$

where

I is the number of photons that reaches the detector per unit time after passing through a soil sample of thickness X,

I_0 is the number of photons that reaches the detector per unit time in the absence of soil for the same distance X between source and detector,

μ_W and μ_S are the attenuation coefficients of the gamma rays by water and soil, respectively, and are specific for the energy of the gamma rays of the source used,

d_S is the soil bulk density (g cm^{-3}),

and θ is the water content (cm^3 cm^{-3}).

Since only part of the interaction is described by eq. (54), calibration curves for such neutron/gamma probes are established experimentally using the model presented above for backscattering. In this case, the count ratio, CR, includes the back-scattered and the transmitted photons. Parameters *A*, *B* and *C* are obtained from measurements in materials of known thickness and density, as in Table XIV and Fig. 10.

Similar to the measurement of bulk density of a moist soil by backscattering, some of the photons not counted by the detector are due to attenuation by the soil water. From these measured values of wet bulk density, the dry-soil bulk density can be obtained using eq. (53).

3.3. Calibration

Due to the relative complexity of calibration, most neutron/gamma probes have factory settings stored in the microprocessor. Calibration for density determination is complex because, a) they require the use of standardized blocks of special materials of various densities, and b) the parameters of the mathematical model are difficult to obtain. Only when appropriate facilities are available can factory calibrations be modified or recalculated by the user. Some models of probes with mathematical processors allow calibration if a set of standard blocks is available to the user. For such a calibration, blocks of at least three different densities (low, medium and high) and two different **equivalent water contents**[1] (low and high) are required. It is sometimes possible also to modify the values of the parameters in the calibration equations stored in the microprocessor, to obtain a better relationship between readings and measured values.

Some probes provide an opportunity to store correction coefficients to automatically adjust calibration for specific soil conditions. For example, water content is overestimated in soils that are high in organic-matter, in calcareous compounds, or in hydrogen sources other than water. For automatic correction of water content in such soils, the deviation from the probe reading in relation to the real value measured in the laboratory by gravimetric methods is introduced into the memory of the microprocessor. Such corrections can be used to adjust the factory calibration, regardless of the cause of the observed systematic differences. It is possible also to substitute the equation furnished by the manufacturer for water content without causing changes in the equation for bulk density, as recommended previously for depth probes.

Table XIV shows the contents of the memory in a microprocessor of a surface neutron/gamma probe, related to its calibration for density: a) counting of photons (gamma rays) at various depths of the gamma source in three standard media of known density, b) standard counting for density (photon counting in the standard position over a standard block that belongs to the equipment), c) values of the coefficients *A*, *B* and *C* for calibration eq (51) for the different depths, d) date of calibration, and e) date of the standard count (optional).

[1]Equivalent water content refers to materials of known hydrogen content, equivalent to a given water content, for reasons of neutron moderation.

TABLE XIV. MICROPROCESSOR MEMORY CONTENT OF CPN PROBE MODEL MC-3, WITH RESPECT TO DENSITY CALIBRATION

Depth	Standard density count: 37,426 / Date of calibration: 23/09/1996					
	Counts at density of (g cm^{-3})			Equation coefficients		
(cm)	1.72	2.14	2.63	A	B	C
BS[a]	27,159	20,136	14,882	2.96	1.03	0.169
AC[b]	54,791	40,970	29,425	4.88	1.38	0.0681
5.0	137,842	102,072	70,641	12.1	1.63	– 0.493
7.5	136,354	98,474	65,574	12.9	1.56	– 0.625
10.0	127,121	88,344	57,156	14.4	1.23	– 0.177
12.5	113,500	75,368	46,739	16.0	1.04	– 0.0158
15.0	97,338	62,090	36,633	16.0	0.954	– 0.0304
17.5	80,888	49,047	27,488	16.7	0.840	0.0108
20.0	65,356	37,486	20,262	18.4	0.718	0.0741
22.5	51,567	28,224	14,730	18.5	0.649	0.0761
22.5	51,567	28,224	14,730	18.5	0.649	0.0761
25.0	40,144	21,170	10,764	17.4	0.603	0.0674
27.5	30,940	15,776	8,083	17.6	0.546	0.0758
30.0	23,728	11,953	6,165	15.0	0.526	0.0648

[a]Backscattering, a little above the soil surface.
[b]Asphalt-concrete, at the soil surface.

Figure 9 shows the calibration curves of the probe when operating at positions BS and AC (Table XIV), which allow density measurements of thin surface layers when drilling a hole for introduction of the rod is not feasible. Figure 10 shows the calibration for operation positions ranging from 5 to 30 cm. In this case the value of the density corresponds to the soil sample crossed by the gamma beam, that is, between source and detector, and both phenomena, backscattering and attenuation, play a role in the measurements.

Table XV shows the contents of the memory of the microprocessor of a surface neutron/gamma probe in relation to its calibration for soil water-content: a) standard count for water content (count of slow neutrons at the standard position over a standard block that belongs to the equipment), b) date of the standard count, c) date of calibration, d) counts of slow neutrons for standard blocks of known equivalent water contents, and e) values of coefficients *A* and *B* of the calibration equation for water content. As is the case for all depth neutron probes, the calibration is the linear model, $\theta = A + B \times CR$ in which θ is the volumetric soil-water content (cm^3 cm^{-3}) and *CR* is the relative count rate [see eq. (5)].

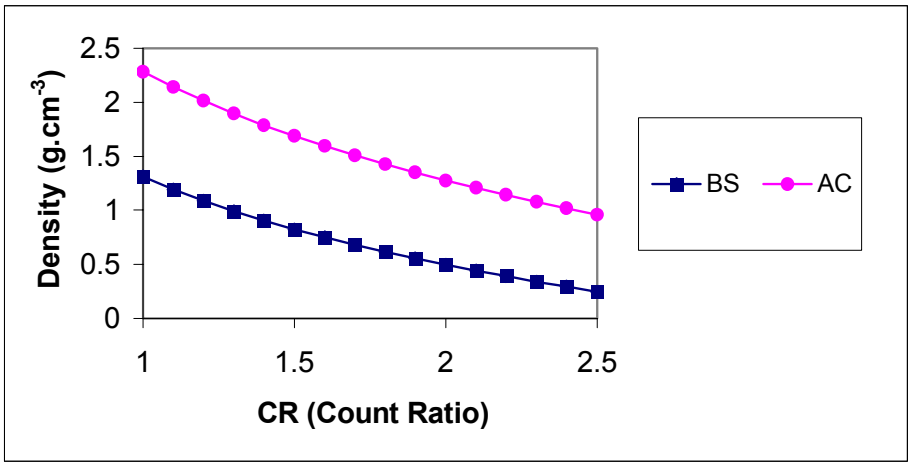

FIG. 9. Calibration curves of a probe for measuring density of a porous medium utilizing gamma ray backscattering.

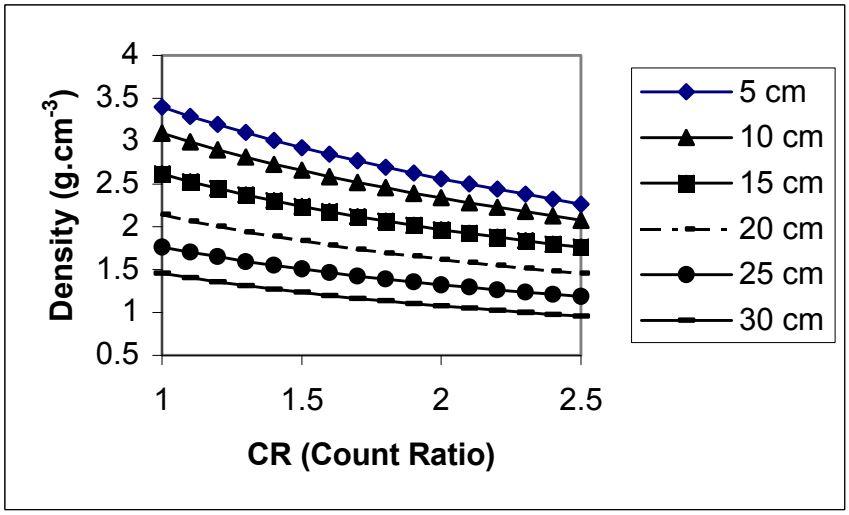

FIG. 10. Calibration curves of a probe measuring density of a porous medium utilizing gamma ray attenuation and backscattering, through various soil thickness.

TABLE XV. CONTENTS OF THE MEMORY OF THE MICROPROCESSOR OF A CPN PROBE, MODEL MC-3, WITH RESPECT TO CALIBRATION FOR SOIL-WATER CONTENT

Standard count for water content: 8,344, date: 23/09/96			
Count for		Calibration coefficient	
$\theta = 0$ cm^3 cm^{-3}	$\theta = 0.53$ cm^3 cm^{-3}	*A*	*B*
337	5263	– 0.03627	0.90265

4. APPLICATIONS

4.1. Soil-water storage

Further to the discussion in Section 2.6.3, we now give a practical example. The water stored in a soil between depths z_1 and z_2 at time t is defined as

$$S_{z_2-z_1}(t) = \int_{z_1}^{z_2} \theta(z,t)\, dz \tag{55}$$

where

θ is the volumetric water content given by eq. (2) ($cm^3\ cm^{-3}$),
and z is the vertical-position coordinate, from the surface (cm).

Since θ is expressed as cm^3 of water per cm^3 of soil, S becomes equivalent to a column of water. Each cm of stored water corresponds to a volume of 10 L per m^2 of soil surface. The most common case is when $z_1 = 0$ (soil surface) and the integration is made over the entire soil profile to depth z_2.

It was shown in Section 2.6.3.3. that the numerical method adopted to determine the integral in eq. (55) has little influence on estimated value of water storage. Equation (37), which is used in the trapezoidal method, may be simplified by assuming that the water profile is a sequence of equal layers, thus $\theta(z, z + \Delta z) = \theta(z + \Delta z)$ if the measurements are spaced at Δz. With this simplification, eq. (37) becomes

$$S_{z_2} = \sum_{i=0}^{n-1} \theta_{i+1} \times \Delta z = \left[\theta_1 + \ldots + \theta_i + \ldots + \theta_{n-1} + \theta_n\right] \times \Delta z \tag{56}$$

where

$$S_{z_2} = n \times \bar{\theta} \times \Delta z = \bar{\theta} \times z_2 \tag{57}$$

if $\bar{\theta}$ is the average water content on n measurements made every Δz from depth Δz in the profile (θ, z_2). Table XVI shows an example of field data from which water storage is estimated below using eq. (57).

TABLE XVI. COUNT RATIOS AND WATER CONTENTS AS A FUNCTION OF SOIL DEPTH FOR A CORN CROP ON AN ALFISOL, PIRACICABA, BRAZIL

Depth (cm)	Count ratio (CR)	Water content ($cm^3\ cm^{-3}$)
25	0.494	0.420
50	0.485	0.410
75	0.503	0.429
100	0.473	0.398
125	0.465	0.389
150	0.471	0.396

Using eq. (67), the following soil-water storage data are calculated with little difficulty:

S_{150-0} = 0.407(150 – 0) = 61.1 cm or 611 mm
S_{75-0} = 0.420(75 – 0) = 31.5 cm or 315 mm
S_{100-50} = 0.412(100 – 50) = 20.6 cm or 206 mm

It is important to know the sphere of influence of the probe, especially for measurements close to the surface. In the present example, it has a radius of approximately 15 cm; therefore, with the probe at 25 cm, the count is influenced by moisture from 10- to 40-cm depth. Because we are not measuring the water content in the top 10 cm of soil, this introduces an error using eq. (57) in the calculation of water storage near the surface, hence it is advisable to make surface measurements by gravimetric means. On the other hand, the measurement at 25 cm is accurate because neutrons did not escape from the surface.

The neutron probe averages the distribution of moisture over the volume of the sphere of influence. Figure 11 illustrates averaging for the data in Table XVI; the shaded areas demonstrate how the spheres of influence overlap. It is appropriate that the probe provides an average measure of water content because, indeed, calculations made with eq. (57) are based on average values. When probe measurements are made with spheres of influence closely overlapping, the accuracy of determination of the total amount of water in the profile is improved.

In this example, had measurements been taken at 10-cm intervals, a better estimate of water stored in the 150-cm soil profile would have been obtained. However, for such a sampling program, care is needed near the soil surface: a measurement at 10 cm would result in part of the sphere of influence being above the soil.

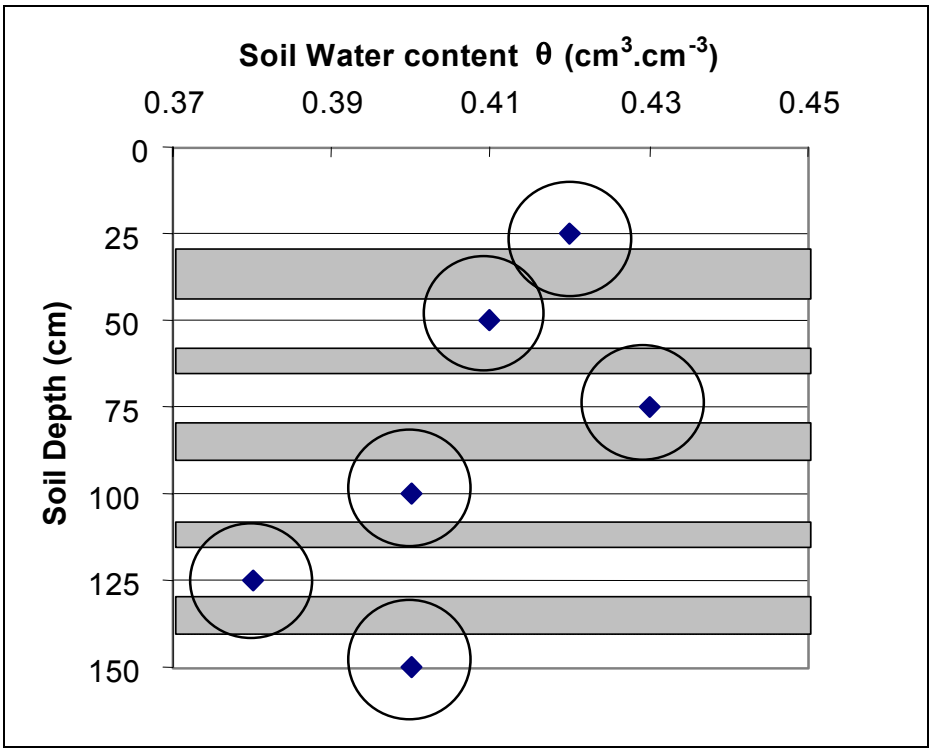

FIG. 11. Soil water content profile (Table XVI data) determined with a neutron probe.

Modern neutron probes have microprocessors that calculate automatically the soil-water storage in mm of water or other appropriate units. Others, still more sophisticated, move up and down in the access tube at a constant speed, obtaining excellent integration of the moisture distribution, and providing a single count rate representing the amount of water in the profile.

Another important aspect is **monitoring changes with time**. As moisture is gained from rainfall or irrigation, or lost by evapotranspiration or internal drainage, soil-water storage fluctuates as a function of time.

Example: For the same corn crop, neutron-probe measurements made at different dates gave the following storages:

S_{0-150}(07/09/98) = 611.0 mm
S_{0-150}(14/09/98) = 579.5 mm
S_{0-150}(21/09/98) = 543.8 mm
S_{0-150}(28/09/98) = 575.8 mm

There was no rain or irrigation during the period 7–21/09. The average rates of water loss, as evapotranspiration and drainage below 150 cm were

$$\frac{\partial S}{\partial t} \approx \frac{S_{0-150}(14/9) - S_{0-150}(7/9)}{14-7} = -4.5 \text{ mm d}^{-1}$$

$$\frac{\partial S}{\partial t} \approx \frac{S_{0-150}(21/9) - S_{0-150}(14/9)}{21-14} = -5.1 \text{ mm d}^{-1}$$

These data alone preclude drawing distinction between evapotranspiration and drainage loss. There was rain during the period 21–28/09, hence water storage increased with an average rate of

$$\frac{\partial S}{\partial t} \approx \frac{S_{0-150}(28/9) - S_{0-150}(21/9)}{28-21} = 4.6 \text{ mm d}^{-1}$$

This increase was the net result of rainfall exceeding combined losses from runoff, evapotranspiration, and drainage below 150 cm.

4.2. Field soil-water retention curves

Field water-retention curves are established by combining neutron-probe readings with those from tensiometers taken at the same time and soil depth. The tensiometers should be installed close to access tubes just outside the "sphere of influence" of the probe. If installed too close to an tube, the water in the tensiometer cup interferes significantly with probe function. A distance of 20 to 30 cm is adequate.

The physical properties of field soils can be variable over even relatively small distances. Owing to spatial variability of their field soils, Villagra et al. (1988) and Greminger et al. (1985) had difficulty ascertaining accurate and precise soil-water-retention curves (Fig. 12). The IAEA (1984) presented an average water-retention curve obtained with tensiometers and neutron probes for soils of several countries (Fig. 13).

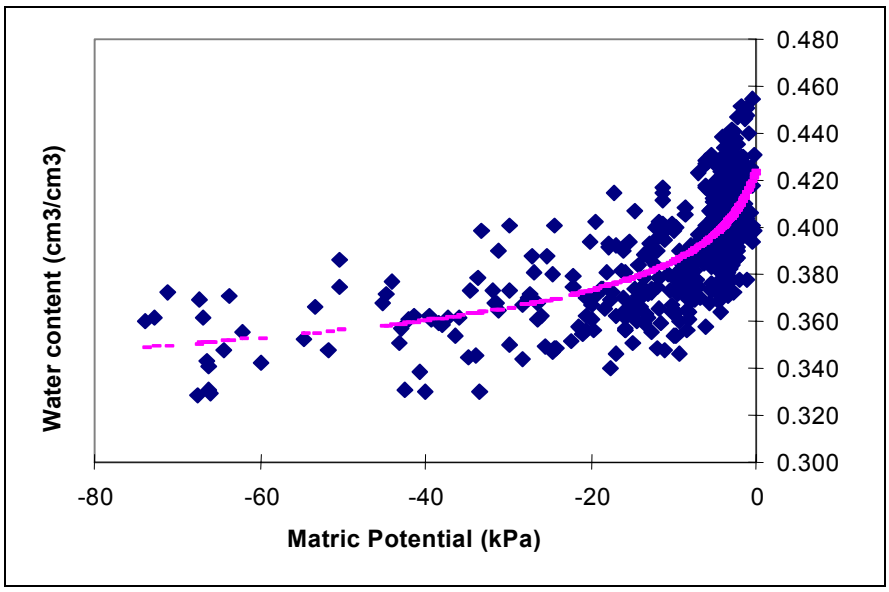

FIG. 12. Soil-water retention curve for an Alfisol at 20 cm (Villagra et al., 1988).

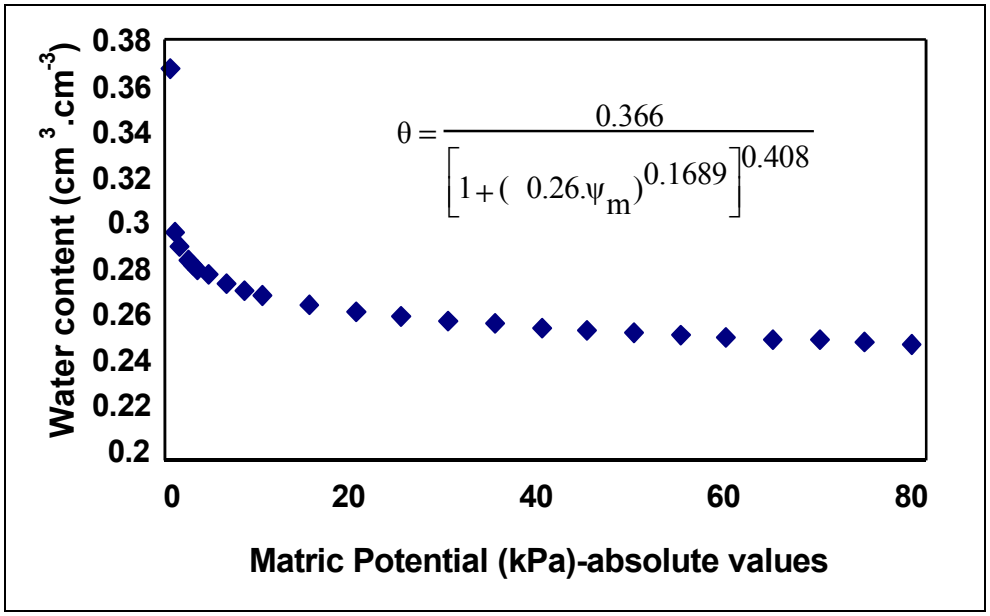

FIG. 13. Average water-retention curve for field soils of several countries (IAEA, 1984).

4.3. Soil hydraulic conductivity

Soil hydraulic conductivity, K, is a parameter that indicates the ability of a soil to transmit water. Because it is strongly dependent on water content, θ, we define the function $K(\theta)$ for each soil. Hence, all methods used to measure hydraulic conductivity require the measurement of moisture content, for which the neutron probe is especially convenient and appropriate for field conditions. As examples, we discuss the methods of Richards et al. (1956), Libardi et al. (1980), and Sisson et al. (1980).

To determine experimentally the $K(\theta)$ function, access tubes and tensiometers are installed down to the desired depths in a level field plot of at least 9 m^2 and generally less than 100 m^2. Water is continuously ponded on its surface to a minimum depth until infiltration reaches an approximate steady-state condition. This condition is also signalled by neutron-probe readings that are constant with time and soil-water contents that approach maximum relative values at each depth within the profile. The steady-state rate of infiltration into the soil surface is recorded and assumed equal to the hydraulic conductivity, K_0, of the topsoil corresponding to the soil-water content θ_0 of the topsoil during the time of steady infiltration. The most commonly used function of $K(\theta)$ is

$$K(\theta) = K_0 \exp[\gamma(\theta - \theta_0)] \tag{58}$$

where

γ is determined from measurements taken after infiltration and during the time water redistributes and drains from the soil in the absence of roots and evaporation (cm cm^{-3}).

After infiltration, when water is no longer applied to the plot and the standing water is absorbed, the surface is covered with plastic to prevent evaporation, and periodic measurements of water content and water matric potential are taken at selected depths with a neutron probe and tensiometers, respectively. Considering that the soil-water redistribution process begins at $t = 0$ (the moment at which water is no longer ponded on the plot), measurements of water content, $\theta(z, t)$, such as those given in Table XVII, are obtained. Simultaneous measurements of matric potential, $\psi_m(z, t)$, are corrected for the corresponding depths (z) (gravitational potential) to obtain values of the total soil-water potential, $\psi_T(z, t) = (\psi_m(z, t) + z)$, such as those given in Table XVIII.

The value for saturated hydraulic conductivity K_0 measured during steady-state infiltration was 2.2 cm d^{-1}. This value together with those of $\theta(z, t)$ and $\psi_T(z, t)$ presented in Tables XVII and XVIII, respectively, will be used in calculations of $K(\theta)$ by the following three methods.

TABLE XVII. SOIL-WATER CONTENTS DURING REDISTRIBUTION

Depth	Soil-water content θ (cm^3 cm^{-3})				
(cm)	$t = 0$	$t = 1$ d	$t = 3$ d	$t = 7$ d	$t = 15$ d
0	0.500	0.463	0.433	0.413	0.396
30	0.501	0.466	0.432	0.414	0.398
60	0.458	0.405	0.375	0.347	0.307
90	0.475	0.453	0.438	0.423	0.414
120	0.486	0.464	0.452	0.440	0.427

TABLE XVIII. TOTAL SOIL-WATER POTENTIAL HEAD DURING REDISTRIBUTION

Depth	Soil-water potential ψ_T (cm H_2O)				
(cm)	$t = 0$	$t = 1$ d	$t = 3$ d	$t = 7$ d	$t = 15$ d
15	– 18	– 38	– 69	– 100	– 135
45	– 47	– 76	– 104	– 129	– 164
75	– 76	– 105	– 135	– 163	– 200
105	– 108	–141	– 172	– 206	– 229
135	– 140	– 172	– 201	– 240	– 265

4.3.1. Method of Richards et al. (1956)

The drainage-flux method proposed by Richard et al. (1956), was developed further by Nielsen et al. (1964), Rose et al. (1965), and van Bavel et al. (1968). It is now recognized as the **instantaneous-profile method** (Watson, 1966) and is used to determine the hydraulic conductivity of well drained soils. It is assumed that the rate of decrease of water stored in a profile for $0 = z = L$, during redistribution in the absence of evaporation and water absorption by plant roots, is equal to the soil-water flux density at depth L, which, according to Darcy's law, may be expressed as:

$$q_L = -K[\theta(L)] \times \left(\frac{\partial \psi_T}{\partial z} \right)_L \tag{59}$$

Water content variation is given by

$$\frac{\partial S(L,t)}{\partial t} = \frac{\partial}{\partial t} \int_0^L \theta(z,t) \times dz = \int_0^L \frac{\partial \theta(z,t)}{\partial t} \times dz \tag{60}$$

From eqq. (59) and (60) as assumed with the method of Richards, we finally obtain the hydraulic conductivity equation:

$$K[\theta(L)] = \frac{\int_0^L \frac{\partial \theta(z,t)}{\partial t} dz}{\frac{\partial \psi_T}{\partial z}} = \frac{\frac{\partial S(L,t)}{\partial t}}{\frac{\partial \psi_T}{\partial z}} \tag{61}$$

The integral is evaluated by first calculating the water stored $S(L, t)$ using eq. (57) for each measurement time. The derivative of $S(L, t)$ can be approximated using the change in water storage for a given time period. Or, the values of $S(L, t)$ from eq. (57) can be used in a regression equation of the form $S(L,t) = a + b \ln t$, where $\partial S/\partial t = q_L = 1/b$. The total water-potential gradient $\partial \psi_T/\partial z$ is estimated from the differences in potentials between two adjacent depths.

Example: The soil-water content data in Table XVII are converted to soil-water storage $S(L, t)$ using eq. (57) for values of $L = 30$, 60, 90 and 120 cm.

Depth L (cm)	Soil-water storage $S(L,t)$				
	$t = 0$	$t = 1$ d	$t = 3$ d	$t = 7$ d	$t = 15$ d
30	150.2	139.4	129.8	124.1	119.1
60	291.8	266.8	248.0	234.8	220.2
90	435.2	402.1	377.6	359.3	340.9
120	580.8	540.2	511.2	488.9	466.1

With these $S(L, t)$ data, values of their time derivatives are estimated from

$$\frac{\partial S(L,t)}{\partial t} = \frac{S(L,t_{i+1}) - S(L,t_i)}{t_{i+1} - t_i} \tag{62}$$

or from the derivative of the regression equation $S(L,t) = a + b \ln t$ for each depth L:

Depth L (cm)	Change in water storage $\frac{\partial S(L,t)}{\partial t}$ (mm d^{-1})			
	$t = 0.5$	$t = 2$	$t = 5$	$t = 11$
30	–10.8	–4.8	–1.4	–0.6
60	–25.0	–9.4	–3.3	–1.8
90	–33.1	–12.3	–4.6	–2.3
120	–40.6	–14.5	–5.6	–2.9

Comparing Tables XVII and XVIII, it is noteworthy that the depths of the tensiometer readings were different from those at which water content, θ, was measured. Those differences allow the total water-potential-head gradient to be estimated at the depth at which θ was measured. As an example, values of the total water-potential head at depths of 45 and 75 cm were used to estimate the gradient at L = 60 cm. In general terms, the gradient is estimated as follows:

$$\frac{\partial \psi_T(L,t)}{\partial z} = \frac{\psi_T[L_{j+1},t] - \psi_T[L_{j-1},t]}{(L_{j+1} - L_{j-1})} \tag{63}$$

Because the values of water flux density at depths L in the above table are average values between times t_i and t_{i+1}, it is necessary to calculate the average values of total soil-water-potential head $\overline{\psi}_T$ from values of ψ_T given in Table XVIII for times t_i and t_{i+1}.

$$\overline{\psi}_T\left[L, \frac{t_i + t_{i+1}}{2}\right] = \frac{\psi_T[L,t_i] + \psi_T[L,t_{i+1}]}{2} \tag{64}$$

A new table of data is obtained:

Depth (cm)	Total water potential $\overline{\psi}_T$ [L,$(t_i+t_{i+1})/2$] (cm H_2O)			
	t = 0.5 d	t = 2 d	t = 5 d	t = 11 d
15	–28.0	–53.5	–84.5	–117.5
45	–61.5	–90.0	–116.5	–146.5
75	–90.5	–120.0	–149.0	–181.5
105	–124.5	–156.5	–189.0	–217.5
135	–156.0	–186.5	–220.5	–252.5

The hydraulic gradients are calculated using the above values for $\overline{\psi}_T$ using eq. (63):

Depth L (cm)	Hydraulic gradient $\partial\psi_T/\partial z$ [cm cm^{-1}]			
	t = 0.5 d	t = 2 d	t = 5 d	t = 11 d
30	–1.117	–1.217	–1.067	–0.967
60	–0.967	–1.000	–1.083	–1.167
90	–1.133	–1.217	–1.333	–1.200
120	–1.050	–1.000	–1.050	–1.167

We obtain values for hydraulic conductivity by dividing the soil-water flux density by the respective hydraulic gradient.

Depth L (cm)	Hydraulic conductivity K [mm d^{-1}]			
	t = 0.5	t = 2	t = 5	t = 11
30	9.67	3.95	1.34	0.64
60	25.86	9.40	3.05	1.56
90	29.18	10.08	3.42	1.92
120	38.63	14.52	5.31	2.44

To construct the function *K(θ)*, we must know the water-content values. The measurement of θ were made at t_i= 0, 1, 3, 7, and 15 days (Table XVII) and we need to estimate them at t_i' = 0,5, 2, 5, and 11 days. As already made for the water-storage [eq. (62)], values of $\overline{\theta}$ corresponding to the above values for K are estimated by linear interpolation to provide the arithmetic means of the values of θ given in Table XVII.

Depth L (cm)	Interpolated water content $\theta(L,t)$ (cm^3 cm^{-3})			
	t = 0.5 d	t = 2 d	t = 5 d	t = 11 d
30	0.484	0.449	0.423	0.406
60	0.432	0.390	0.361	0.327
90	0.464	0.446	0.431	0.419
120	0.475	0.458	0.446	0.434

Hence, values of K, corresponding to θ for each soil depth L, are:

L = 30 cm		L = 60 cm		L = 90 cm		L = 120 cm	
θ	K	θ	K	θ	K	θ	K
0.484	9.67	0.432	25.86	0.464	29.18	0.475	38.63
0.449	3.95	0.390	9.40	0.446	10.08	0.458	14.52
0.423	1.34	0.361	3.05	0.431	3.42	0.446	5.31
0.406	0.64	0.327	1.56	0.419	1.92	0.434	2.44

For each soil depth L, a regression of ln$K$ versus θ is made to ascertain the appropriateness of assuming the functional relationship given by eq. (58).

Depth L (cm)	Regression: ln$K$ = a + b × θ		
	a	b	R^2
30	–14.591	35.112	0.985
60	–8.708	27.748	0.987
90	–24.980	61.123	0.996
120	–28.467	67.731	0.995

In view of the high values of R^2, it is justified to assume that the relation between K and θ is exponential. Using eq. (58), it can be verified that the parameter b of the regression line ln $K = a + b \times \theta$ is identical to γ, whereas K_0 is related to the parameters a and γ by $K_0 = \exp [a + \gamma \times \theta_0]$ where θ_0 is the water content at $t = 0$. Finally, the estimated parameters according the model of eq. (58) are as follows:

L (cm)	Model, eq. (58): $K = K_0 \exp [\gamma \times (\theta - \theta_0)]$		
	K_0 [mm d^{-1}]	γ	θ_0
30	20.08	35.112	0.501
60	54.65	27.748	0.458
90	57.61	61.123	0.475
120	85.62	67.731	0.486

Owing to the fact that K is an exponential function of θ, small errors in θ lead to large errors in K.

4.3.2. Method of Libardi et al. (1980)

This method is based on the additional hypothesis that the gradient of the total water-potential head is does not vary from unity: grad $\psi_T = \partial \psi_T / \partial z = 1$. Thus, eq. (61) becomes simplified because the data obtained from tensiometers shown in Table XVIII are not needed. Combined with model of eq. (58), the integration with time of the simplified eq. (61) becomes:

$$\theta - \theta_0 = -\frac{1}{\gamma} \ln t - \frac{1}{\gamma} \ln \left(\frac{\gamma K_0}{L} \right) \tag{65}$$

Values of K_0 and γ of eq. (58) are obtained from $(\theta - \theta_0) = f(\ln t)$.

Example: For the measured values of θ_0 at time $t = 0$ given in Table XVII, linear regression equations of graphs of $(\theta - \theta_0)$ versus ln t for each depth L were determined.

Depth L (cm)	Regression: $(\theta - \theta_0) = a + b \times \ln t$			
	θ_0	A	b	R^2
30	0.501	–0.0376	–0.0250	0.989
60	0.458	–0.0485	–0.0355	0.976
90	0.475	–0.0218	–0.0147	0.996
120	0.486	–0.0207	–0.0136	0.990

According to eq. (65), the slope $b = \gamma^{-1}$ and the intercept $a = \gamma^{-1} \cdot \ln(\gamma K_0 L^{-1})$. Hence, by the method of Libardi et al. (1980), we have the parameters K_0, γ and θ_0 determined at depths L, as follows.

Depth L (cm)	Model, eq. (58): $K = K_0 \exp[\gamma \times (\theta - \theta_0)]$		
	K_0 (mm d^{-1})	γ	θ_0
30	33.76	40.054	0.501
60	83.59	28.209	0.458
90	58.39	67.945	0.475
120	74.82	73.578	0.486

4.3.3. Method of Sisson et al. (1980)

Because this method also is based on the assumption that the gradient of the total soil-water-potential head is unity, the data obtained from tensiometers shown in Table XVIII are again neglected. Values of K_0 and γ of eq. (58) are obtained directly from graphs of ln (zt^{-1}) versus $(\theta - \theta_0)$ for any given depth L according to

$$\ln(z t^{-1}) = \ln(\gamma K_0) + \gamma(\theta - \theta_0) \qquad (66)$$

Example: For the measured values of θ_0 at $t = 0$ given in Table XVII, linear regression equations of graphs of ln (zt^{-1}) versus $(\theta - \theta_0)$ for depths L are required. The data for those regression calculations for $z = L = 30$ are:

t (d)	L = 30 cm		L = 60 cm		L = 90 cm		L = 120 cm	
	ln(z/t)	$(\theta-\theta_0)$	ln(z/t)	$(\theta-\theta_0)$	ln(z/t)	$(\theta-\theta_0)$	ln(z/t)	$(\theta-\theta_0)$
1	3.4012	–0.035	4.0943	–0.053	4.4998	–0.022	4.7875	–0.022
3	2.3026	–0.069	2.9957	–0.083	3.4012	–0.037	3.6889	–0.034
7	1.4553	–0.087	2.1484	–0.111	2.5539	–0.052	2.8416	–0.046
15	0.6931	–0.103	1.3863	–0.151	1.7918	–0.061	2.0794	–0.059

The results of the regression are:

Depth L (cm)	Regression: $\ln(z/t) = a + b \times (\theta - \theta_0)$			
	θ_0	a	b	R^2
30	0.501	4.8747	39.6139	0.989
60	0.458	5.3961	27.5370	0.976
90	0.475	5.9706	67.6490	0.996
120	0.486	6.2799	72.8095	0.990

According to eq. (66), the intercept $a = \ln(\gamma K_0)$ and the slope $b = \gamma$. Hence, we have the parameters K_0, γ and θ_0 determined at depths L:

Depth L (cm)	Model, eq. (58): $K = K_0 \exp[\gamma \times (\theta - \theta_0)]$		
	K_0 (mm d^{-1})	γ	θ_0 (cm^3 cm^{-3})
30	33.05	39.614	0.501
60	80.09	27.537	0.458
90	57.91	67.649	0.475
120	73.31	72.810	0.486

In summary, it is noteworthy that the results of the latter two methods gave similar values for a given soil depth. Results obtained with the method of Richards et al. (1956) differed from the others owing to the inclusion of the measured values of the hydraulic gradient in the calculations. It is interesting to compare the estimates of K_0 and γ obtained by the different methods. For example, at 90 cm depth, the following values were obtained.

Method	γ	K_0 (mm d^{-1})
Richards et al. (1956)	61.12	57.61
Libardi et al. (1980)	67.95	58.39
Sisson et al. (1980)	67.65	57.91

It is noteworthy that the methods of Libardi et al. (1980) and of Sisson et al. (1980) gave similar values; both are based on the same simplified hypothesis, whereas the method of Richards provided different estimates owing to the inclusion of the measured values of the hydraulic gradient in the calculations. Tensiometer readings are quality data to be preferred in the estimation of the parameters of the hydraulic-conductivity/soil-water-content relationship.

4.4. Water balance

Water balance is a computation of gains and losses to and from an agro-ecosystem over time interval Δt and for a selected soil-layer thickness. Magnitudes both of the time interval, Δt ($t_{final} - t_{initial}$), and soil thickness, L (soil depth z is measured positively downward), depend on the objectives of the investigation. The most commonly used values of Δt are a few days, a week, a month, and a year. The value of L depends on the depth exploited by the roots, and, in

general, is selected to include 95 to 100% of the root system. For a given region, the water balance (Fig. 14) is given by

$$P + I - ET - RO - Q_L = \Delta S_L \qquad (67)$$

where

P is the rainfall integrated over Δt (mm),
I is the irrigation integrated over Δt (mm),
ET is the evapotranspiration integrated over Δt (mm),
RO is the runoff integrated over Δt (mm),
Q_L is the water draining from the soil at depth L integrated over Δt (mm),
and ΔS_L is the change in soil-water storage in layer $(0, L)$ during the interval Δt (mm).

All of the above values are expressed in equivalent water-layer thickness (mm). The signs in eq. (67) have been selected so that they are normally expressed by a positive or null value. Thus, P, I, and ET are normally positive or zero.

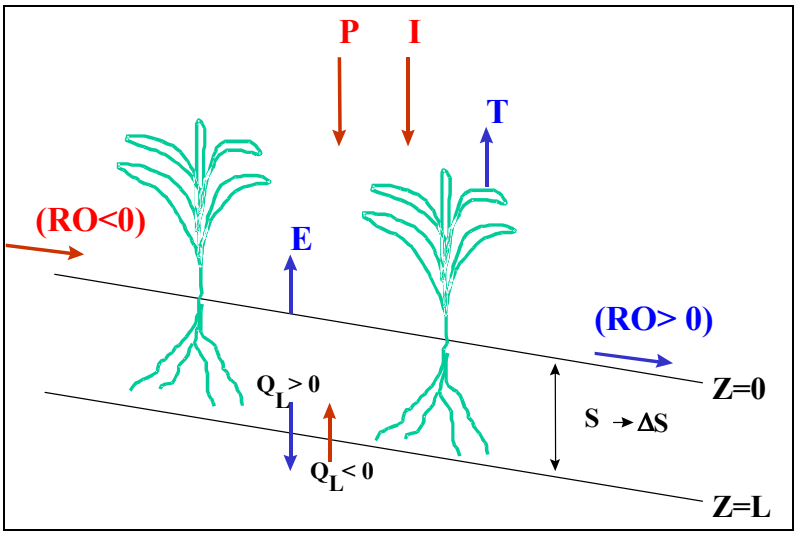

FIG. 14. Water-balance components.

It is noteworthy that, if water runs onto the soil, the magnitude of RO is negative and contributes positively to ΔS_L. Also, if the magnitude of Q_L is negative, water moves upward into the profile and contributes positively to ΔS_L; a positive value for Q_L indicates drainage from the profile. A positive value for ΔS_L denotes a positive balance and an increase in soil-water storage in the profile $(0, L)$; ΔS_L <0 shows a negative balance.

Neutron probes are well suited for water-balance studies because the measurements they provide facilitate the calculation of soil-water storage, S_L, and changes thereof, ΔS_L, for various depths in soil profiles. The method is non-destructive, and many measurements may be made at a single location, as necessary. Below are examples, based on eq. (67).

Example 1: In Fig. 14, we assume that the soil profile has 280 mm of water and receives 10 and 30 mm rainfall and irrigation, respectively. Evapotranspiration amounts to 40 mm. If RO and Q_L are neglected, what would be the final soil-water storage?

$$P + I - ET - RO - Q_L = \Delta S_L = 10 + 30 - 40 - 0 - 0 = 0 \text{ mm.}$$

Therefore, because $S_L(t_{final}) = S_L(t_{initial}) + \Delta S_L$, the final storage $S_L(t_{final})$ would be 280 + 0, i.e. 280 mm.

Example 2: Without rainfall and irrigation, what would be the change in soil-water storage if evapotranspiration losses are 35 mm and the drainage at depth *L* is 8 mm?

$$P + I - ET - RO - Q_L = \Delta S_L = 0 + 0 - 35 - 0 - 8 = -43 \text{ mm}$$

Therefore, the storage would decrease by 43 mm of water.

Example 3: Considering evapotranspiration as negligible through a cloudy period during which a plot receives 56 mm of rain, what would be the change in soil-water storage if 14 mm of water are lost through run-off and the soil profile loses 5 mm by drainage?

$$P + I - ET - RO - Q_L = \Delta S_L = 56 + 0 + 0 - 14 - 5 = 37 \text{ mm}$$

Therefore, storage would increase by 37 mm.

Example 4: Assuming that no water drains from the profile during a period without precipitation, what would be the amount of water received by a crop through irrigation if evapotranspiration amounted to 42 mm and storage decreased 12 mm?

$$P + I - ET - RO - Q_L = \Delta S_L = 0 + I - 42 - 0 - 0 = -12$$

Therefore, the crop was irrigated with 30 mm of water.

Example 5: During a 10-d period with rainfall of 15 mm, a farmer irrigated his bean crop with two 10-mm applications. If, during that same period, soil-water drainage was 2 mm and the water in the soil profile decreased 5 mm, what would be the daily evapotranspiration rate of the field crop?

$$P + I - ET - RO - Q_L = \Delta S_L = 15 + 20 - ET - 0 - 2 = -5$$

Therefore, with evapotranspiration of 38 mm during the 10-d period, the *ET* would be 3.8 mm d^{-1}.

4.4.1. Estimating components of the water balance

Measuring the individual components of the water balance is somewhat troublesome. The rainfall, *P*, measured in mm·d^{-1} with various types of rain gauges, is usually integrated over the period Δt in days to obtain the total amount of precipitation in mm. Because precipitation is non-uniform over a region, rain gauges should be installed close to the area for which the water balance is to be estimated. Reichardt et al. (1995) have discussed spatial and temporal variability of rainfall distribution on a 1,000-ha scale.

Measuring the amount of water applied by irrigation, *I*, at a particular location in a field also poses a challenge for the investigator. Owing to sprinkler variability, many samples are necessary to ascertain the distribution. In the case of furrow or other forms of surface

irrigation, a simple estimate obtained by dividing the total volume of applied water by the irrigated area fails to take account of variability in spatial distribution.

Oftentimes, evapotranspiration, *ET*, is treated as unknown in the water-balance equation and calculated from the other components, as in *Example 5*. *ET* can be estimated from theoretical and/or empirical equations based on atmospheric data using the methods of Thornwaite, Blaney-Criddle and Penman. It can be estimated also with lysimeters (FAO, 1992).

Run-off, *RO*, is difficult to measure. In fact, it is commonly estimated only from measurements taken on standardized plots of various soil types and slopes. The information from such standardized plots is extrapolated to other locations where water-balance studies are being conducted. For example, if 35 mm or rain on a standard plot (2 m wide and 22 m long) resulted in 216 L of water being collected at the downhill end of the plot, the run-off would be

$$RO = \frac{216\times10^{3}\ \text{cm}^{3}}{2\times22\times10^{4}\ \text{cm}^{2}} = 0.491\,\text{cm or } 4.91\,\text{mm} = \frac{4.91}{35} \approx 14\%\ \text{of the rainfall}$$

Hence, for a water-balance study on the same soil and slope, runoff would be assumed to be 14% of the rainfall. This simple calculation ignores the fact that water lost from higher elevations is gained at lower elevations.

Soil-water flux, Q_L, at the bottom of a soil profile at depth L at a given location within a field or watershed is usually estimated for a time interval ($t_{i+1} - t_i$) by

$$Q_L = \int_{t_i}^{t_{i+1}} q_L\,dt \tag{68}$$

where

q_L is the soil-water flux at depth L given by Darcy's equation [eq. (59)]:

$$q_L = -K_L(\theta)\frac{\partial\psi_T(L)}{\partial z}$$

with z increasing positively downward. The gradient ($\partial\psi_T / \partial z$) indicates the direction and intensity of the soil-water flux. If the term is negative, the flux is positive water moves downward (draining from the soil profile) at $z = L$. A positive value indicates that the flux is negative and water is moving upward and entering the bottom of the profile at $z = L$. To calculate the rate at which water is moving requires a knowledge of the hydraulic conductivity, $K(\theta)$, of the soil**.** Its determination using neutron probes was discussed in Section 4.3.

Example: For a field soil profile of z = 100 cm, assume that the hydraulic conductivity is described by $K(\theta)$ = 5.68 exp[85.6(θ – 0.441)] mm d^{-1}. The soil-water content, θ, measured with a neutron probe at z = 100 cm, was 0.398 cm^3 cm^{-3}. If the matric-potential head measured with tensiometers at 90 and 110 cm was –118 and –135 cm, respectively, what would be the direction and magnitude of the soil-water flux at the bottom of the profile? The pertinent calculations are as follows:

– For $\theta = 0.398$ cm^3 cm^{-3}, the value of the hydraulic conductivity is 0.143 mm d^{-1}.
– For $z = 90$, $\psi_T = \psi_m - z = -118 - 90 = -208$ cm
– For $z = 100$, $\psi_T = \psi_m - z = -135 - 110 = -245$ cm
– $\frac{\partial \psi_T}{\partial z} \approx \frac{\psi_T(110) - \psi_T(90)}{110 - 90} = \frac{-245 - (-208)}{20} \approx 1.85$
– From eq. (59), $q_L = -0.143 \times (-1.85) \tilde{} 0.265$ mm d^{-1}.

Thus, qL is positive, denoting a downward flow of water out of the profile at a rate of 0.26 mm·d^{-1}. If this value of drainage persisted for 5 days, we would have $Q_L = 0.26 \times 5 = 1.3$ mm.

The calculations to estimate the variation in water storage ΔS_L have been given in detain in Section 4.1.

Further information on water balance can be found elsewhere (IAEA, 1990), and in publications by Villagra et al. (1988) and Bacchi et al. (1996) for applications under Brazilian conditions.

4.5. Spatial variability of soil

The neutron probes is very useful for analysing the distribution and spatial variability of water content within fields and watersheds. Using a large number of sampling points and analyzing the spatial and temporal variances with theories of regionalized variables, a better understanding of processes associated with soil-water transfer can be achieved. Studies can be performed with a variety of sampling schemes such as sampling locations being equally or randomly spaced in transects or grids.

Figure 15 shows neutron-probe measurements of soil-water contents taken on three dates along a transect of twenty-five access tubes located at 5-m intervals. The trends of variation along the transect were similar for each of the sampling dates, verifying that the neutron probe sampled the same location at each time point (Reichardt et al., 1993; Reichardt et al., 1997).

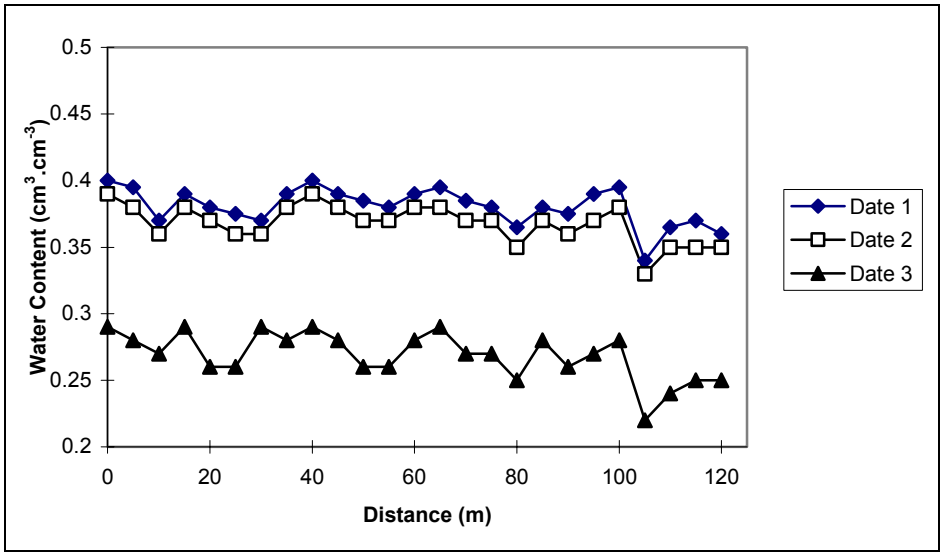

FIG. 15. Soil-water content measured on three dates along a 125-m transect.

4.6. Water extraction by roots

Neutron probes can be used also to examine patterns of moisture extraction by plant roots. Figures 16 and 17 show the results obtained in a study to assess the water extraction by the root system of a rubber plantation (Mendes et al., 1992). Combining neutron (soil-water content) and tensiometer (total water-potential head) measurements at different locations allowed the mapping of soil-water status through the construction of isolines of soil-water content, θ, and total water-potential head, ψ_T. The lines of water flux, q – perpendicular to the lines of total water potential – can be observed: water flux is oriented towards the decreasing values of total water potential. Although precise quantification of those fluxes remains difficult, this mapping allowed spatial characterization of water extraction by the roots of the trees, and monitoring of seasonal variation.

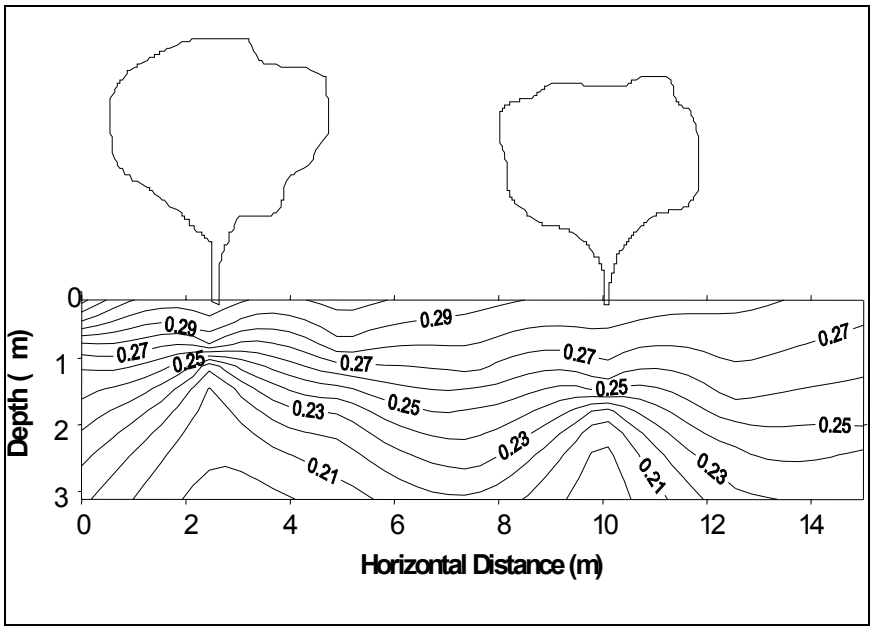

FIG. 16. Isolines of soil-water content beneath two rubber trees.

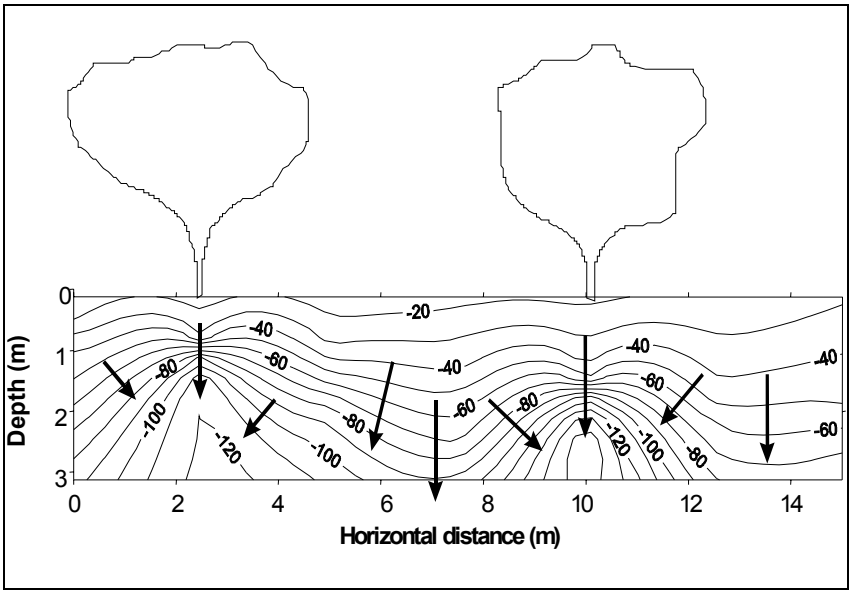

FIG. 17. Isolines of total soil-water-potential head and flow direction lines beneath two rubber trees.

4.7. Irrigation control

Where water resources are scarce, it is important to control all aspects of irrigation. It is necessary not only to preserve irrigation water, but also to guarantee its efficient use by crops. Specialized publications deal in detail with irrigation methods; the reader may consult the FAO Technical Bulletin series "FAO Irrigation and Drainage Papers. This manual covers basic concepts relating to the use of neutron and gamma probes. As noted previously, the neutron probe is an excellent device for measuring soil-water content and for the estimation of water stored to a given depth (Section 4.1.). Thus, the neutron probe can be used to control soil-water content in experiments designed to measure impact of deficit irrigation on crop yields (Calvache and Reichardt, 1996; Kirda et al., 1999). However, the main questions relating remain the same: **when**, **how**, and **how much** to irrigate? We will develop basic concepts to assist in addressing these questions rationally, with practical examples.

4.7.1. Estimation of irrigation depth

Irrigation depth, which depends on the rooting depth of a crop, is defined as the quantity of water (mm) to be applied to a soil.

The **net irrigation depth**, I_N, is the quantity of water applied to a soil, which is expected to be totally used by the crop through evapotranspiration. It does not include losses by drainage and excessive evaporation in the absence of complete crop cover. The procedures commonly used to calculate the net irrigation depth are, 1) an edaphic or soil procedure, and 2) an analytical procedure based on the actual evapotranspirationof the crop calculated from the water balance discussed in Section 4.4.

The edaphic procedure assumes that, after rain or irrigation, the amount of water held in the soil against the force of gravity is defined as field capacity, θ_{FC}. Several additional assumptions not stated in this definition are that the soil is deep and permeable, no evaporation occurs from the surface and no water table or slowly permeable barriers occur at shallow depths in the profile. In a few days after infiltration under these conditions, it is assumed that the rate of redistribution of water within the profile will decrease sufficiently to be considered nil, and that any further reduction in the water content will occur only through uptake by roots. Hence, this "upper" limit of storage is used to calculate net irrigation depth.

This procedure assumes also that a "lower" limit of water storage exists, below which plant roots can no longer extract moisture. This lower limit is the permanent wilting percentage, θ_{PWP}. The mere presence of water held between θ_{FC} and θ_{PWP} is not sufficient without further assuming that the soil must be interlaced with a density of plant roots sufficient to extract moisture down to the θ_{PWP}. Because the rooting depth of an annual crop changes with time, especially early in the growing season, it is important also to recognize that the net irrigation depth is not constant. Nevertheless, the edaphic procedure provides useful general guidelines for ascertaining the net irrigation depth.

The best estimate of θ_{FC} is made directly in the field after irrigation, using a neutron probe to estimate the water content after redistribution ceases. Estimates are made also using soil samples analyzed in the laboratory to determine their water content when their matric potential is between –30 and –10 kPa. Estimates of θ_{PWP} are routinely measured in the lab on initially water-saturated soil samples subjected to a matric potential of –1500 kPa.

Hence, for a field soil with a water content equal to the θ_{PWP}, the net irrigation depth, I_N, measured in mm, is based on the equation:

$$I_N = (\theta_{FC} - \theta_{PWP}) \times L \tag{69}$$

where

I_N is the net irrigation depth,
θ_{FC} is the soil-water content at field capacity,
θ_{PWP} is the soil-water content at permanent wilting percentage,
L is the depth (mm) to which the soil is to be watered.

On the other hand, it is sometimes advisable to irrigate a crop before the soil-water content is reduced to θ_{PWP}, in order to avoid physiological disorders associated with stress from lack of moisture. In those cases, the net irrigation depth is based on the equation:

$$I_N = (\theta_{FC} - \theta_{critical}) \times L \tag{70}$$

where

$\theta_{critical}$ is the lowest soil-water content ($cm^3\ cm^{-3}$) that does not cause physiological disorders in the plants in question, and is defined by

$$\theta_{critical} = \theta_{FC} - f(\theta_{FC} - \theta_{PWP}) \tag{71}$$

where

f is the **irrigation criterion** defining the permissible water consumption or the fraction of permissible water consumption (Doorembos and Kassam, 1986).

*Examples:*A crop of beans is growing in a soil of the following properties:

Depth (cm)	θ_{CC} ($cm^3\ cm^{-3}$)	θ_{PFP} ($cm^3\ cm^{-3}$)
0 – 20	0.30	0.18
20 – 50	0.28	0.19
50 – 80	0.27	0.19

Example: Assuming the initial soil-water content is the θ_{PWP}, calculate the net irrigation depth for the bean crop assuming that the roots are distributed to a depth of 0.8 m, to return to field capacity.

Because the soil is stratified, the net irrigation depth is calculated separately for each layer according to eq. (75):

For layer 1, $I_N = (0.30 - 0.18) \times 200 = 24$ mm
For layer 2, $I_N = (0.28 - 0.19) \times 300 = 27$ mm
For layer 3, $I_N = (0.27 - 0.19) \times 300 = 24$ mm

Hence, the total net irrigation to achieve the rooting depth of 0.8 m would be 75 mm.

Example: Assuming that the bean crop's roots extend to only 0.5 m, and that the irrigation criterion is 0.4, calculate the net irrigation requirement.

Values of $\theta_{critical}$ are calculated according to eq. (71) for each soil layer having roots:

For layer 1, $\theta_{critical} = 0.30 - 0.4(0.30 - 0.18) = 0.252$ ($cm^3\ cm^{-3}$)
For layer 2, $\theta_{critical} = 0.28 - 0.4(0.28 - 0.19) = 0.244$ ($cm^3\ cm^{-3}$)

The net irrigation depth is calculated separately for each layer according to eq. (70):

For layer 1, $I_N = (0.30 - 0.252)\times 200 = 9.6$ mm
For layer 2, $I_N = (0.28 - 0.244)\times 300 = 10.8$ mm

Hence, the total net irrigation for the rooting depth of 0.5 m would be 20.4 mm.

Gross irrigation depth is the amount of water required for the crop, the net irrigation depth, plus the additional water needed to offset losses associated with the particular kind of irrigation method. Table XIX provides a range of typical values of application efficiencies for three kinds of irrigation methods.

TABLE XIX. APPLICATION EFFICIENCIES OF IRRIGATION METHODS (Doorembos and Pruitt, 1992)

Irrigation method	Efficiency
Furrow	0.6–0.7
Sprinkler	0.8–0.9
Drip	0.9–0.95

Furrow irrigation results in water loss from conveyance ditches as well as excessive application to the upper ends of the furrows. Drip irrigation, the most efficient, requires the most energy.

Gross irrigation depth I_G is based on the equation:

$$I_G = \frac{I_N}{IE} \tag{72}$$

where

I_N is net irrigation depth,
and IE is the irrigation application efficiency (< 1).

Values of gross irrigation are given not only in depth of water (mm), but also in terms of volume (V) or out-flow of water on the area of the field and the time allowed for application, the "irrigation period," which is defined as follows:

$$V = Q \times t = A \times I_G \tag{73}$$

where

Q is the out-flow ($L\ s^{-1}$),
A is the irrigated area (m^2),
and t is the period of irrigation (s).

A noteworthy rule of thumb is that 1 mm of irrigation water equals 1 L m^{-2}.

Example: Assuming an irrigation efficiency of 0.9, use eq. (72) to calculate the gross irrigation depth for the bean crop in the above example with roots distributed to a depth of 0.8 m.

I_G = 75/0.9 = 83 mm

Example: Assuming an irrigation efficiency of 0.9, use eq. (72) to calculate the gross irrigation depth for the bean crop in the above example with roots distributed to a depth of only 0.5 m.

I_G = 20.4/(0.9) = 23 mm

Example: For a gross irrigation depth of 16 mm, use eq. (73) to calculate the irrigation period for a water out-flow of 0.27 m^3 s^{-1} onto an area of 5 ha.

$t = A \times I_G \ / \ Q$ = (50,000 m^2)×(16 L m^{-2}) / (270 L s^{-1}) = 2,963 s or 49.4 min

4.7.2. Irrigation frequency

When and how often a farmer should irrigate are major questions. The frequency of irrigation is commonly estimated by two methods.

4.7.2.1 Empirical method

The empirical method for calculating the irrigation frequency, *IF*, is based on actual evapotranspiration, ET_a (the consumptive use of water by the crop), and the net irrigation depth capable of being stored by the soil. Values of ET_a are estimated usually from direct methods of field-water balance or theoretical/empirical methods like those of Penman or Blaney-Criddle. Irrigation frequency is calculated according to

$$IF = \frac{I_N}{ET_a} \tag{74}$$

where

ET_a is the average daily consumptive use during the selected period (mm).

Example: Assume that the daily water consumption rate of a snap-bean crop during flowering is 4 mm d^{-1}. If the net irrigation depth applied to the soil during this period is 40 mm, calculate the irrigation frequency.

According to eq. (74),

IF = (40 mm)/(4 mm d^{-1}) = 10 d

Hence, irrigation should be applied at intervals of 10 d.

4.7.2.2. Practical method

This method is based on daily field measurements. It differs from the empirical method in that it takes into account the distribution of natural rainfall across the field as well as variations associated with local soil and crop conditions. Daily determinations of soil-water content with neutron probes at various depths are made to estimate water storage within the rooting depth. Also, tensiometers and other measuring devices are frequently used to assess the local conditions within the field.

Once the first irrigation is accomplished, neutron-probe readings are collected daily to assess the real water storage. Often, this is accomplished by tensiometer readings also. The next irrigation is made when the average water content reaches a critical value defined in eq. (71), representing the least amount of water in the profile that the crop is able to use without stress or alteration of any physiological process that would affect crop quality or yield. With this value estimated in advance, irrigation is applied considering the net and gross depths given by eqq. (70) and (72), respectively (Doorembos and Kassam, 1986; Calvache and Reichardt, 1996).

4.7.3. Evaluation of irrigation systems

Parameters used to evaluate the performance of irrigation systems are based on the uniformity of the application and the amounts of loss by deep drainage, run-off and evaporation. Parameters commonly used to evaluate irrigation systems are: a) irrigation efficiency, b) efficiency of use of irrigation water, c) uniformity of distribution, and d) efficiency of soil-water storage. An evaluation of each of these parameters is easily made through the use of the neutron probe to ascertain water content and storage.

4.7.3.1. Irrigation efficiency

The irrigation or application efficiency, *IE*, is the ratio of the average depth of water applied and stored in the root zone as a result of an irrigation to the gross irrigation depth or the total water delivered by the distribution system. Irrigation efficiency is calculated according to

$$IE = \frac{I_N}{I_G} \tag{75}$$

where

IE is < 1 and usually expressed as %.

Example: Assuming that, after a field has been irrigated with a gross water depth of 100 mm, the amount stored in the soil is 80 mm, calculate the irrigation efficiency from eq. (75).

IE = (80 mm)/(100 mm) = 0.8 or 80%.

4.7.3.2. Efficiency of use of irrigation water

The efficiency of use of irrigation water, *EUIW*, is the ratio of the evapotranspiration depth summed over the entire crop-growth cycle to the summed net irrigation depth of water applied. Hence, the efficiency of use of irrigation water is defined as:

$$EUIW = \frac{ET_a}{I_N} \tag{76}$$

where

EUIW is < 1 and usually expressed as %.

Example: During the production of a bean crop, assume that the evapotranspiration was 500 mm as a result of applying a net irrigation depth of 700 mm of water during the season. According to equation (76), what was the efficiency of use of irrigation water?

EUIW = (500 mm)/(700 mm) = 0.71 or 71%.

4.7.3.3. Uniformity of water distribution during irrigation

Several expressions are used to define how uniform is the distribution of irrigation within a field. Here, we present commonly used ratios to quantify it: a) uniformity of water distribution during furrow irrigation, b) Christiansen's uniformity coefficient, and c) efficiency of stored irrigation water.

– The **uniformity of water distribution** during furrow or border irrigation, *DU*, is the ratio of the average depth of irrigation water infiltrated and stored in the root zone of the lowest quarter area of the field to the average depth of irrigation water applied over the entire area of the field.

$$DU = \frac{\text{average depth of irrigation water infiltrated in the lowest quarter of the field}}{\text{average depth of irrigation water applied to the entire field}} \tag{77}$$

Example: if the average infiltrated water depth of the lower quarter of a furrow field was 30 mm and that of the entire field was 40 mm, then

DU = (30 mm)/(40 mm) = 0.75 or 75%.

– **Christiansen's uniformity coefficient**, *UC*, is a measure of the variability of the amount of water storage within the field as a result of an irrigation. It is defined by

$$UC = 1 - \left(N \times \overline{S}_L\right)^{-1} \sum_{i=1}^{N} \left| S_{L_i} - \overline{S}_L \right| \tag{78}$$

where

S_{L_i} is defined by eq. (56) as the soil water stored at location *i* to depth *L* (mm), and $\overline{S}_L$ the average of all locations *N*.

Example: if the sum of the absolute values of the deviations of ten measurements of irrigation water storage is 5 mm, and the field average of the stored water is 50 mm, the value of *UC*, according to eq. (78), is $1 - (10 \times 50 \text{ mm})^{-1}(5 \text{ mm}) = 0.999$ or 99.9%.

– **Relative irrigation water stored**, *RS*, is a commonly used term for evaluating the amount of water potentially able to be stored in an individual irrigation system. It can serve also as an indicator of the effectiveness of irrigation, because it expresses the quantity of irrigation water that entered into, and was stored by, the soil as a result of one or more irrigations. It is defined by

$$RS = \frac{\overline{S}_L}{\overline{\theta}_{FC} \times L} = \frac{\overline{S}_L}{(\overline{S}_L)_{\max}} \tag{79}$$

where

$\overline{S}_L$ and $(\overline{S}_L)_{\max}$ are the average water storage depth (mm), and the maximum possible average water storage depths, respectively.

Example: If the average stored water depth in an irrigated field was 60 mm and the maximum possible average storage is 70 mm, then, according to eq. (79),

RS = (60 mm)/(70 mm) = 0.86 = 86%.

These efficiency and uniformity parameters help to evaluate and improve the design of an irrigation system as well as maintain its performance.

In conclusion, we stress again that all of these parameters can be rapidly and reliably quantified under field conditions using the neutron probe.

4.8. Control of soil compaction

Farmers, agricultural scientists and engineers have long recognized the detrimental effects of compaction, particularly after irrigation of fields of fine-textured soils. Growers are especially concerned because the deleterious effects worsen with time and reduce crop yields. And, the use of heavy machinery exacerbates the problem. Soil compaction increases the cost of production owing to the need for new, more expensive management procedures, including sub-soiling. Sugar-cane production in Brazil provides an excellent example of soil deterioration and crop-production losses owing to compaction. Huge mechanical harvesters and trucks have replaced manual, traditional non-compacting harvesting procedures. The damaging effects on soil are frequently observed through not only decreases in productivity but also decreases in number of economically viable ratoon crops. Eventually, severely compacted fields must be sub-soiled with deep tines drawn by heavy, caterpillar-treaded tractors, at high operational cost.

Efficient techniques for monitoring and ultimately controlling compaction in various cropping systems have long been the focus of agricultural researchers, particularly those in soil physics, soil mechanics and agricultural engineering. For them, neutron/gamma probes have proven to be of great value for simultaneous measurements of soil-water content and bulk density.

Figure 18 shows a surface neutron/gamma probe in a Brazilian sugarcane field. Data in Table XX indicate that the equipment is adequate for monitoring soil bulk-density changes caused by mechanized harvesters and heavy transport vehicles.

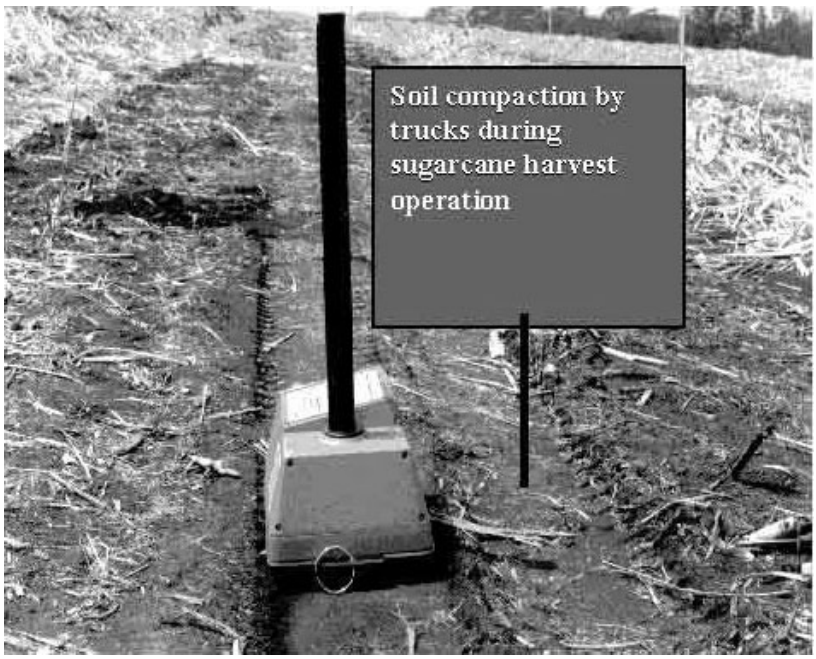

FIG. 18. Evaluation of soil compaction in a sugarcane field by use of a surface neutron/gamma probe.

TABLE XX. CHANGES IN SOIL BULK DENSITY AFTER HARVEST AND EFFECTS OF TRANSPORT IN A SUGAR-CANE FIELD

Layer (cm)	Soil bulk density (g cm^{-3})			
	Primary forest	Sugar cane field		
		Before harvest	After harvest	After transport
0–2.5	0.943	1.247	1.384	1.481
0–5.0	0.995	1.355	1.441	1.528
0–7.5	1.070	1.436	1.450	1.558
0–10.0	1.130	1.463	1.496	1.552
0–12.5	1.132	1.477	1.503	1.560

Large agricultural enterprises are now adopting neutron/gamma probes for routine evaluation of soil water and bulk density prior to harvest operations. These evaluations identify times when fields can be harvested with minimal soil compaction from heavy vehicles. Neutron/gamma probes are being used also to identify times when specific regions of a field require sub-soiling operations.

BIBLIOGRAPHY

ARSLAN, A., et al., The performance and radiation exposure of some neutron probes in measuring the water content of the topsoil layer, Aust. J. Soil Res. **35** (1997) 1397–1407.

BACCHI, O.O.S., et al., Balanço hídrico em cultura de aveia forrageira de inverno na região de São Carlos, S.P., Sci. Agric. **53** (1996) 172–178.

CALVACHE, A.M., REICHARDT, K., Efeito de épocas de deficiência hídrica na eficiência do uso de nitrogênio na cultura de feijão cv. Imbabello, Sci. Agric. **53** (1996) 343–353.

CARNAHAN, B., et al., Applied Numerical Methods, John Wiley, New York (1969) 604 pp.

CARNEIRO, C., DE JONG, E., In situ determination of the slope of the calibration curve of a neutron probe using a volumetric technique, Soil Sci. **250** (1985) 250–254.

COUCHAT, P.H., et al., "The measurement of thermal neutron constants of the soil: application to the calibration of neutron moisture and the pedological study of the soil", Nuclear Cross Sections Technology (SCHRACH, R.A., BOWMAN, C.D., Eds.), NBS SP 425, Washington, DC (1975).

DOOREMBOS, J., KASSAM, A.H., Yield Response to Water, FAO Irrigation and Drainage Paper 33, FAO, Rome (1986) 193 pp.

DOOREMBOS, J., PRUITT, W.O., Crop Water Requirements, FAO Irrigation and Drainage Paper 24, FAO, Rome (1992) 144 pp.

FALLEIROS, M.C., Medida da Umidade do Solo Com Conda de Neutrons, PhD Thesis, Instituto de Pesquisas Energéticas e Nucleares, Universidade de São Paulo/CNEN (1994).

FOOD AND AGRICULTURE ORGANIZATION, Crop Water Requirements, FAO Irrigation and Drainage Paper Nº 24, FAO, Rome (1992).

FOOD AND AGRICULTURE ORGANIZATION OF THE UNITED NATIONS, INTERNATIONAL ATOMIC ENERGY AGENCY, INTERNATIONAL LABOR ORGANIZATION, OECD NUCLEAR ENERGY AGENCY, PAN AMERICAN HEALTH ORGANIZATION, WORLD HEALTH ORGANIZATION, International Basis Safety Standards for Protection Against Ionizing Radiation and for the Safety of Radiation Sources, Safety Series No. 115, IAEA, Vienna (1996a).

FOOD AND AGRICULTURE ORGANIZATION OF THE UNITED NATIONS, INTERNATIONAL ATOMIC ENERGY AGENCY, INTERNATIONAL LABOR ORGANIZATION, OECD NUCLEAR ENERGY AGENCY, PAN AMERICAN HEALTH ORGANIZATION, WORLD HEALTH ORGANIZATION, Radiation Protection and the Safety of Radiation Sources, Safety Series No. 120, IAEA (1996b).

GREACEN, E.L., Soil Water Assessment by the Neutron Method, CSIRO, Adelaide (1981) 140 pp.

GREMINGER, P.J., et al., Spatial variability of field measured soil water characteristics, Soil Sci. Soc. Am. J., **49** (1985) 1075–1082.

GRIMALDI, C., et al., The effect of the chemical composition of a ferralitic soil on neutron probe calibration. Soil Tech. **7** (1994) 233–247.

GUZMÁN, J., Nucleonica Basica, Segunda Edicion, Centro de Documentacion e Informacion Nuclear del Instituto de Asuntos Nucleares, Bogotá (1989) 312 pp.

HAVERKAMP, R., et al., Error analysis in estimating soil water content from neutron probe measurement: 1. Local standpoint, Soil Sci., **137** (1984) 78–90.

INTERNATIONAL ATOMIC ENERGY AGENCY, Neutron Moisture Gauges, IAEA, Vienna (1970).

INTERNATIONAL ATOMIC ENERGY AGENCY, Tracer Manual on Crops and Soils, Technical Reports Series No. 171, IAEA, Vienna (1976).

INTERNATIONAL ATOMIC ENERGY AGENCY, Field soil-water properties measured through radiation techniques, Technical Reports Series No. 312, IAEA, Vienna (1984).

INTERNATIONAL ATOMIC ENERGY AGENCY, Use of nuclear techniques in studies of soil-plant relationships, Training Course Series No. 2, IAEA, Vienna (1990).

INTERNATIONAL ATOMIC ENERGY AGENCY, INTERNATIONAL LABOR ORGANIZATION, Occupational Radiation Protection, Safety Standards Series No. RS-G-1.1. IAEA, Vienna, (1999).

KIRDA, C., et al., (Eds.), Crop Yield Response to Deficit Irrigation, Kluwer Academic Publishers, Dordrecht (1999).

KLUTE, A., Methods of Soil Analysis, Part 1, Physical and Mineralogical Methods, Second Edition, Agronomy Monograph series No. 9, ASA and SSSA, Madison (1986) 1188 pp.

KUTILEK, M., NIELSEN, D.R., Soil Hydrology, Catena-Verlag, Cremlingen-Destedt (1994) 370 pp.

LIBARDI, P.L., et al., Simplified field methods for estimating the unsaturated hydraulic conductivity, Soil Sci. Soc. Am. J. **44** (1980) 3–6.

MENDES, M.E.G., et al., Relações hídricas em seringal no município de Piracicaba, Sci. Agric. **49** (1992) 103–109.

NIELSEN, D.R., et al., Water movement through Panoche clay loam soil, Hilgardia **35** (1964) 491–506.

OLGAARD, P.L., Problems Connected with the Use of Subsurface Neutron Moisture Gauges and their Solution, Riso-M980 20, Danish Atomic Energy Commission, Copenhagen (1969) 20 pp.

ORESEGUN, M.O., "Radiation safety of soil neutron moisture probes", Comparison of Soil Water Measurement Using the Neutron Scattering, Time Domain Reflectometry and Capacitance Methods, IAEA-TECDOC-1137, IAEA, Vienna (2000), 139–146.

REICHARDT, K., et al., Hydraulic variability in space and time in a dark red latosol of the tropics, Geoderma **60** (1993) 159–168.

REICHARDT, K., et al., Variabilidade diária da chuva em uma escala local (1000 ha) em Piracicaba, S.P., e suas implicações na recarga da água do solo, Sci. Agric. **52** (1995) 43–49.

REICHARDT, K., et al., Correção da calibração de sonda de nêutrons por meio de parâmetros de estabilidade temporal da distribuição de probabilidade do conteúdo de água no solo, Sci. Agric. **54** (1997) 17–21.

RICHARDS, L.A., et al., Physical processes determining water loss from soil, Soil Sci. Soc. Am. Proc. **20** (1956) 310–314.

ROSE, C.W., et al., Determination of hydraulic conductivity as a function of depth and water content for soil in situ, Aust. J. Soil Res. **3** (1965) 1–9.

SISSON, J.B., et al., Simple method for predicting drainage from field plots, Soil Sci. Soc. Am. J. **44** (1980) 1147–1152.

VACHAUD, G., et al., Comparison of methods of calibration of a neutron probe by gravimetry or neutron capture model, J. Hydrol. **34** (1977) 343–356.

VAN BAVEL, C.H.M., et al., Hydraulic properties of a clay loam soil and the field measurement of water uptake by roots: 1. Interpretation of water content and pressure profiles, Soil Sci. Soc. Am. Proc. **32** (1968) 310–317.

VAUCLIN, M., et al., Error analysis in estimating soil water content from neutron probe measurements: 2. Spatial standpoint, Soil Sci. **137** (1984) 141–148.

VILLAGRA, M.M., et al., Tensiometry and spatial variability in Terra Roxa Estruturada, R. Bras. Ci. Solo, **12** (1988) 205–210.

VILLAGRA, M.M., Difficulties of estimating evapotranspiration from the water balance equation, Agr. Forest Meteorol. **72** (1995) 317–325.

WATSON, K.K., An instantaneous profile method for determining the hydraulic conductivity of unsaturated porous materials, Water Resour. Res. **2** (1966) 709–715.

LIST OF CONTRIBUTORS

Main Authors

O.O. Bacchi, Universidade de Sao Paulo, CENA, Piracicaba, SP, Brazil
K. Reichardt, Universidade de Sao Paulo, CENA, Piracicaba, SP, Brazil
M. Calvache, Comisión Ecuatoriana de Energía Atómica, Quito, Ecuador

Peer Reviewers

D. Nielsen, University of California, Davis, United States of America
G. Vachaud, University of Grenoble, LTHE/IMG, France

Technical Editors/Verification of Translations

– English Version
A. Eaglesham, Manuscript Service, Ithaca, United States of America
P.M. Chalk, International Atomic Energy Agency

– Spanish Version
S. Urquiaga, EMBRAPA, CNPAB, Seropedica, RJ, Brazil
F. Zapata, International Atomic Energy Agency

– French Version
J.-P. Laurent, J.L. Thony, & M. Vauclin, University of Grenoble, LTHE/IMG, France
P. Moutonnet, International Atomic Energy Agency

Overall Co-ordinator

F. Zapata, International Atomic Energy Agency